Fluidized Bed Combustion of High-Volatile Fuels

March, 2008

Graduate School of Science and Technology
Niigata University

Winaya, I Nyoman Suprapta

CONTENTS

ABSTRACT

This study is about research on fluidized bed combustion (FBC) of high-volatile fuels. The research has been conducted in five chapters. In the first chapter, literature survey concerning to the problems associated with fluidized bed combustion of high-volatile fuel are summarized. Rapid volatile matter (VM) evolution from fuels such as wastes and biomass is one of problems of fluidized bed incinerators and gasifiers. When VM evolves rapidly in the vicinity of the fuel feed point, the mixing of VM with reactant gas is poor thus unreacted matter is anticipated to be released from the reactor. One of the counter measures to solve this problem is by employing porous solids as bed material.

The second chapter deals with reduction of VM evolution rate by employing porous solids as bed materials instead of non-porous sand. Effect of bed material on the onset of devolatilization was measured by use of a bench-scale bubbling fluidized bed reactor. VM capture by the porous solids (capacitance effect) and heat transfer rate within the bed, both of which affect VM evolution rate, were also measured. Four types of porous solids, with capacitance effect and without capacitance effect, were employed as bed material. By employing porous solids without capacitance effect, the contribution of reduced heat transfer rate and capacitance effect to the delay of VM evolution can be separately evaluated. For porous bed materials with moderate capacitance effect (VM capture of up to 20 %), the delay of the onset of devolatilization, which was measured by detecting the flame combustion of the VM, was well explained by the lower heat transfer between fuel and bed. However, for a porous particle with high capacitance effect (VM capture of 30 %), capacitance effect also affected the delay of the onset of flame combustion.

The third chapter is concerned with a new method to evaluate horizontal dispersion. A carbon-loaded bed material prepared using the capacitance effect (VM captured by porous particles) is used as a tracer. The tracer particles are identical to the remainder of the bed material, except for carbon-loading of a few weight percent. Two carbon-solid tracers were prepared: using a carbon-loaded bed material with dividing bed using a partition plate, and using activated carbon batch injection. Transient change in the horizontal CO concentration profile is measured in the freeboard and the experimental results are compared with the theoretically calculated results of one-dimensional diffusion of solids. Thereby, the horizontal dispersion coefficient is determined. The experimental results agree with results obtained from the literature.

In the fourth chapter of this thesis, a model of combustion and dispersion of carbon deposit on porous bed material during bubbling fluidized bed combustion has been developed. For commercial scale-up purposes, it is important to establish a model in which both carbon deposit (carbon captured by porous bed particles) combustion and horizontal solid dispersion take place simultaneously. The oxidation rate of carbon deposits was measured by burning carbon deposits with oxygen and measuring the produced CO_2. Based on the burning rate of carbon deposits, a one-dimensional mathematical model of carbon deposit combustion in a bubbling fluidized bed was developed. A two-dimensional mathematical model to predict the horizontal concentration profile of carbon combustion was also developed by taking account of both the reaction rate and solid dispersion. The two-dimensional model was validated through experiments using a two-dimensional fluidized bed combustor by continuously feeding solids with carbon deposits into the reactor.

In the fifth chapter, this work is summarized. The works have covered some essential innovations on FBC of high-volatile fuels using porous solids as bed material. The delayed onset of devolatilization is expected to broaden the area of devolatilization in the reactor, thus to avoid formation of local VM-rich zone in the freeboard. A new method has been developed to evaluate horizontal dispersion of solids at high bed temperatures that resemble those of commercial operations. As the first step to scaling-up of the FBC system using carbon loaded solids prepared by capacitance effect, the developed model is considered to be applicable to large-scale BFBCs if the solid dispersion coefficient can be predicted.

Keyword: fluidized bed, volatile matter, porous bed, combustion rate, horizontal dispersion

Chapter 1

General Introduction

1.1 Potential energy of biomass and wastes fuels

The increased efforts of the need to reduce CO_2 emission to prevent global warming from combustion systems have led to an interest in biomass and wastes as fuel sources. As a potentially energy renewable resource, biomass and wastes are gaining more attention worldwide. The use of these fuels to provide partial substitution of fossil fuels has an additional importance to be CO_2 neutral. This is particularly the case with regard to energy plants, which are periodically planted and harvested. During their growth, these plants have consumed CO_2 from the atmosphere for photosynthesis which is released again during combustion. An additional benefit from using wastes as fuels is that the volume of waste is reduced, consequently the need for large landfill areas can be minimized [1].

The biomass can be grouped into the following categories: wood residues, agricultural residues, dedicated energy crops and industrial and municipal waste of plant origin [2]. At present, biomass is converted into heat and electricity most often by combustion and gasification. Biomass and wastes are found in large quantities of residues associated with agricultural residues production such as straw, bagasse,

coffee husks, rice husk, waste woods and processing industries. Unlike fossil fuels which are limited in availability, these resources are not only abundantly available, but also renewable. The production of straw (from cereals like wheat, barley and oat) was distributed fairly uniformly world-wide, both in developing and developed countries, whereas the production of others is predominantly found in the developing countries. Rice husk and straw are the most important agricultural biomass in quantity, amounting to 43% of the total residues [3]. Rice husk is found in over 75 countries where rice is grown and represents, according to variety, 14–35% of the weight of harvested rice [4].

The high energy content in wastes such as plastic wastes can also be used to replace fossil fuels for energy production. Plastic generally has high calorific value products ranging from 18000 to 38000 kcal/kg [5]. The high energy content of plastics as well as the chemical composition of plastics is demanding for alternative treatment of plastic refuses where plastic waste is considered as a resource of energy and as chemical raw material. In the case of wastes, the rapid developments in plastics technology have led the use of plastics in many applications ranging from wrappers to high strength engineered plastic composites for industrial use [6]. The waste arising from this expanding use of plastics is enormous, however only a small percentage have been recycled, while the large majority is landfill or disposal.

Consequently, the responsible for disposal of plastic wastes has created serious social and environmental issues. So, it is expected to decrease in the future since the landfill space is depleted and plastic wastes are resistant to environmental degradation. In addition, recycling is generally used only to produce low grade plastic products, such as, sewer pipes, plastic fencing, industrial plastic pallets, traffic cones, playground equipment and garden furniture [7].

1.2 Characteristic of biomass and wastes fuels

Unlike fossil fuels, some physical and chemical properties of biomass and wastes fuels complicate their processing and combustion. These properties may include moisture content, low bulk density, low melting point of the ash and high content of volatile matter.

In general, moisture content of biomass is higher than coal fuel, however, it can be lower since the crop products like rice, coconuts, groundnuts must be dried before the husks removed. The bulk density of biomass is low that causes a complication of their processing, transportation and combustion [3]. In addition, biomass is relatively rich in alkali and alkaline earth metal, causing it to melt at relatively low bed temperatures which in the worst case may result in total defluidization and unscheduled shutdown [4].

Biomass and wastes are characterized to be high volatile matter (VM) content fuels. The amount of VM which contains in biomass and wastes fuels might range from 60% to 80% and more, compared with a typical figure of 20–30% of medium rank coals [8]. The most of the energy is associated with its volatile content rather than with the solid residue i.e., char.

Water vapor is one of the first volatile components to be produced at just over 100 °C, when a solid fuel is heated gradually up to, e.g., 900 °C. Subsequently, H_2, CO, and CO_2 are produced, together with a wide suite of hydrocarbons, ranging from CH_4 up to tars. Occasionally, soot is generated during devolatilisation; the elements N and S can appear as NH_3, HCN, CH_3CN, H_2S, COS, and CS_2 [9].

In addition, high VM indicates to be easier to ignite and to burn which in turn results in higher combustion efficiency. However, it is difficult to convert the VM in the combustion process since the rapid VM evolution especially near fuel feed point. Efforts must be taken to achieve complete combustion to ensure low emissions of CO and unburned hydrocarbons. Care must also need to handle related to the formation product combustion of gaseous pollutants such as NO_x, SO_2 and N_2O.

1.3 Fluidized bed combustion of high-volatile fuels

Refuse incineration plant is a well-proven and established method to handle the

increasing amount of municipal waste and biomass. The use of fluidized bed combustion (FBC) for waste and biomass incineration has expanded since the twentieth century either for energy recovery or wastes disposal. This technology is well known as one of the promising techniques for its excellent gas-solid mixing and favorable emission characteristics. Pre-processing of biomass/wastes feeds to acceptable particle size and moisture content, usually necessary for conventional technologies, can then be minimized in fluidized-bed operations, as long as it could be conveniently fed into the bed. FBC technology is usually indicated to be the best choice, or sometimes the only choice, to convert alternative fuels to energy due to its fuel flexibility and the possibility to achieve an efficient and clean operation [10]

A great removal and combustion efficiency can be obtained from fluidized-bed combustors. It is also found that a high recovery of heat can be achieved, this is mainly due to the heat transfer coefficient in fluidized bed combustors is much greater than that of conventional combustion systems. However, the high heat transfer means a rapid evolution of VM during heating of feed wastes/biomass. Thus local VM evolution takes place only in the vicinity of the fuel feed point. Due to insufficient mixing of gas in the upper freeboard in fluidized bed combustors, complete combustion is not easy. Often unburned hydrocarbons are released from combustors and it is anticipated that dioxins are formed from such unburned

hydrocarbons if Cl is present. Another problem of local VM evolution is local heat release in the freeboard, which forms locally high temperature region and enhances NO_x formation.

1.4 Counter measures to reduce high-volatile matter evolution

Numerous investigations have been conducted to minimize the harmful of emission and dioxins caused by the high rate of VM evolution. Reducing of bed temperature from the optimum temperature normally used at 1123 K and by minimizing gas superficial into the bed lead to lower a high reaction during coal combustion as reported by Fujiwara *et.al.*, 1995 [11]. Controlling the waste feed rate [12] and introducing baffles in the freeboard [13] enable to enhance the mixing of air to VM. Another possible measure to suppress the rapid VM evolution is the use of a porous bed material that captures hydrocarbons in the pores as a carbon deposit [14-18]. It reduces the amount of evolved VM and increases the conversion of carbon in the dense bed. For that reason, it is expected to enhance the horizontal dispersion of carbonaceous materials by solid mixing in the dense bed. It is also expected to inhibit the formation of local fuel-rich zones as well as high-temperature zones in the freeboard

1.4.1 Reducing of bed temperature

During combustion of biomass and wastes fuels, it was observed a considerable degree of freeboard burning of VM, particularly during over-bed feeding. There was increased freeboard combustion which led to an increase in freeboard temperature within the region near the feed point whereas the dense bed temperature fell as seen in Fig. 1-1.

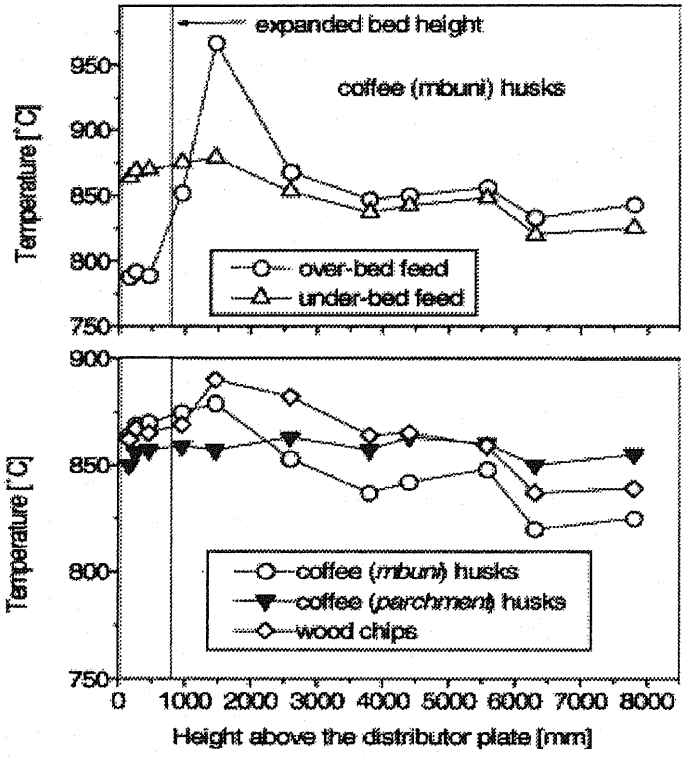

Fig.1-1 The temperature profiles in the FBC combustor during the combustion of biomass [3].

One solution to solve above phenomena is to reduce bed temperature operation of fluidized bed combustion. However, the problem is, while a measure taken to decrease one of the emissions may prove successfully, it has the opposite on one

or two of the others. Bed temperature is undoubtedly as the single most important parameter affecting the rates of formation and destruction emission in fluidized bed combustion. The temperature in the bed is usually maintained at approximately 1123 K so that sulfur capture can be minimized. However, the observation that NO flue gas increases with decreasing bed temperature, while N_2O exhibits an inverse effect.

1.4.2 Providing heating surfaces in the freeboard

Compared with coals, biomass/wastes fuels are characterized by higher contents of volatile matter. This indicates that the residues are easier to ignite and to burn, although the combustion is expected to be rapid and difficult to control. The high volatile matter contents are also expected to affect the overall combustion process. The implication of the high volatile matter contents is that the design and operation principles normally adopted for coal combustion systems, may not be applied for the combustion of biomass/wastes fuels. Care must be taken to achieve complete combustion of the volatiles to ensure higher combustion efficiency and low emissions of CO, hydrocarbons and PAH [8].

Since biomass and wastes are categorized as a high volatile matter fuel, it is required to maintain the bed thermally stable for optimal combustion temperature. In

such a case, the provision of heat transfer surfaces in the above bed zone would be needed, in order to remove excess heat. The location of volatile matter combustion significantly affects the heat release profiles along the combustor. This issue is strictly connected to the extension and location of heat exchange surfaces, to the pathways to pollutants formation, to the reliability and safety of combustor operation.

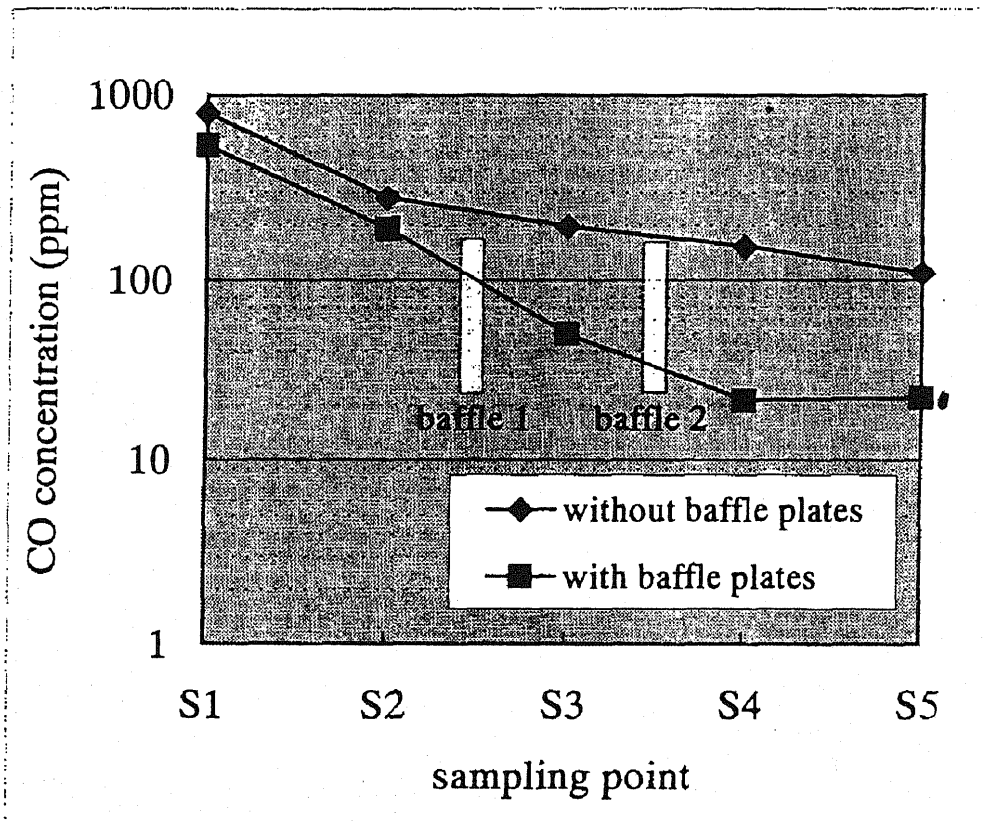

Fig.1- 2. Profiles of temperature as a function of the presence of baffles [13].

The considerations must be taken about quantifying the amount of heat surface required in the freeboard. Little surface would result in excessive temperature in the freeboard and enhance high temperature at the gas exit. However, too much heat

transfer surface may affect ignition process slowing down heat reaction and hence reducing combustion efficiency.

Installing baffles in the freeboard is one of the solutions for this situation [13]. VM combustion significantly affects the heat release profiles along the combustor. By installing baffles in the freeboard, mixing of combustion with VM is enhanced so that the concentration of CO is lower as can be seen on Fig. 1-2.

1.4.3 Air fluidization flow effect

Another important aspect concerning on VMs which are released in the bottom bed and burnt in the freeboard zone is whether the fluidization air flow should be varied. Reduction of gas fluidization velocity into the bed is one of methods to minimize a high rate VM rate, hence to lower emission of unburnt gases [11]. The air flow may be split into two streams, the primary air passing trough the dense bed and the secondary air, perhaps pre-heated or not, being supplied direct to the freeboard. By optimizing secondary air injection [12, 20] enables to enhance mixing of combustion air with volatile matter. Effect of secondary air injection on NO_x concentration in flue gas can be seen in Fig. 3. The addition of secondary air is effective in reducing NO_x levels for refuse derived fuel (RDF). The results indicate that NO_x concentration is higher for RDF-B than that for RDF-A and after the

injection of secondary air, NO_x concentration is reduced greatly. For RDF-A, after the injection of secondary air, NO_x concentration is reduced considerably under high air ratio conditions.

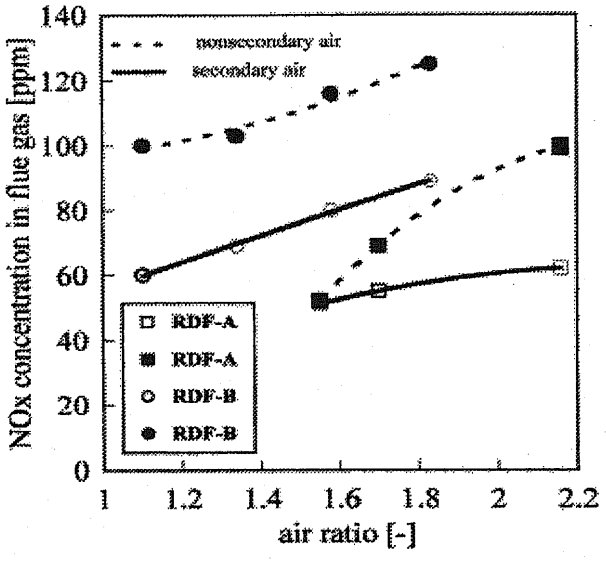

Fig. 1-3. Effect of secondary air injection on No_x concentration in flue gas [20].

An increase on excess air has been generally associated with an increase on the N_2O flue gas. In the case of air staging, however, its influence on the N_2O flue gas does not seem to meet a general consensus. In some cases, the air staging operation results in a decrease on the N_2O flue gas concentration, whereas in other cases the effect seems to be weak and temperature dependent [21,22]. These discrepancies can probably be attributed to local conditions like the temperature, catalytic surfaces, etc.

1.4.4 Employing porous particle as fluidized bed material

One feature of biomass and wastes as a fuel is high VM content. Due to high heat transfer from the bed material to fuel, VM evolution occurs very rapidly when fuel is fed into the bed. Thus local volatile matter evolution takes place only in the vicinity of the fuel feed point. Due to insufficient mixing of gas in the upper freeboard in fluidized bed combustors, complete combustion is difficult to achieve. Often unburned hydrocarbons are released from combustors and it is anticipated that dioxins are formed from such unburned hydrocarbons.

The extensive combustion of volatiles in the freeboard results in higher temperature in the freeboard zone than in bottom bed and a considerable amount of that heat is carried away by the outgoing gas. If the VM are burned in the bed, the heat released mainly absorbed by the bed material. Hence the combustion in the freeboard can be avoided or minimized. A direct consequence of volatiles bypass of the bed from biomass/wastes fuels is that the post combustion of volatiles in the freeboard leads to significant local overheating with respect to the bed.

One of counter measures to solve the above problems in fluidized bed conversion is to employ porous solids as bed material instead of conventional quartz sands. The porous materials capture the VM in their pores in the dense bed as carbon deposit. For a heavy oil cracking process, porous bed materials were

found to capture heavy oil at a temperature range of 690-800 K, as shown schematically in Fig. 4 [9]. Franke et al. (1999) revealed that "capacitance effect" of porous particles occurred under waste incineration conditions at a temperature of 1073 K [14].

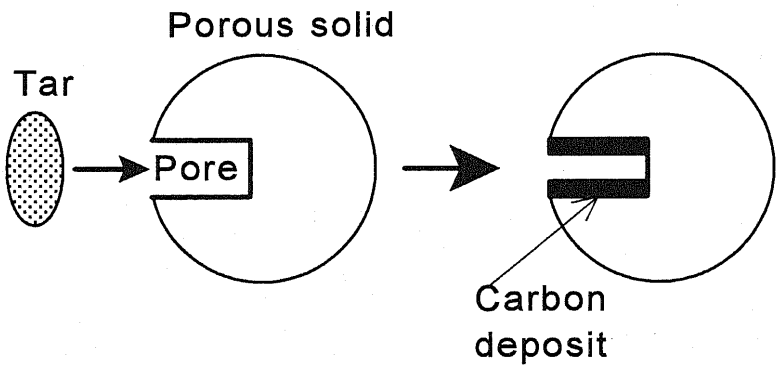

Fig. 1-4. Capacitance effect of porous particle.

Porous bed particles capture volatile matter in the dense bed as carbon deposit in the pores of the porous bed material. When the porous particles were employed into fluidized bed combustion of wastes, the retention of volatile matter in the bottom of bed was increased. The effect of porous bed has been employed for combustion of plastic pellet [24, 25] and for combustion of rice husk [26]. The emissions of hydrocarbons including dioxins were able to reduce. The carbon retention was strongly affected by the type of porous solids. Another advantage of porous bed material is lower heat transfer rate from bed to fuel [27-28]. It moderates the evolution of volatile matter, thus it is expected to inhibit the formation

of local fuel-rich zone as well as high temperature zone.

The porous bed material has also been reported to enhance the horizontal dispersion of carbonaceous material. The horizontal concentration of carbon became uniform and the concentrations of unburnt gaseous became less than those of the conventional sand particle (QS) as seen in Fig. 1-5.

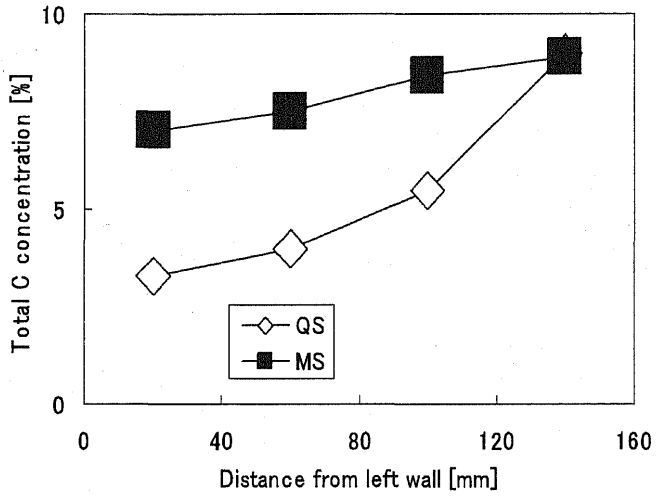

Fig. 1-5. Horizontal concentration profile in the freeboard at 30 cm above distributor [9].

1.5 Concluding Remarks

As reviewed above, this research focuses on fluidized bed combustion of high-volatile fuels such as biomass and wastes. Table 1.1 shows a summary of characteristics of biomass and wastes fuels and their counter measures. The study is emphasized on improvement of carbon burn-up during fluidized bed combustion of high-volatile fuels which includes how to control emission caused by rapid VM

evolution and development of a mathematical model to predict the horizontal concentration profile of carbon deposit combustion by taking account of both the reaction rate and solid dispersion.

In the present study, high VM evolution rate is suppressed by employing porous bed material instead of conventional bed material of quartz sand. Porous bed material has been reported to reduce heat transfer rate and it delayed volatile matter evolution, but the previous works were conducted with capacitance effect. Thus it is possible that the former results of volatile mater evolution were affected by both heat transfer and by capacitance effect. The effect of solely heat transfer rate on volatile matter evolution rate has not yet been fully clarified.

Table 1-1 Characteristics of biomass/wastes fuel with problems and their counter measures

Characteristics	Problems	Counter measure
High volatile matter	- Local volatile matter - High freeboard temperature - Dioxins (PCDDs and PCDFs) - NOx and N_2O formation	- Reducing bed temperature - Controlling the feed wastes - Installing baffles in freeboard - Controlling air fluidization - Employing porous bed material

Porous bed materials capture VM as carbon deposits during fluidized bed combustion of high-volatile fuels. Carbon deposits burn in a dense bed mixed with bed materials; thereby enhancing horizontal dispersion of carbonaceous materials. The schematic diagram is summarized in Fig. 1-6.

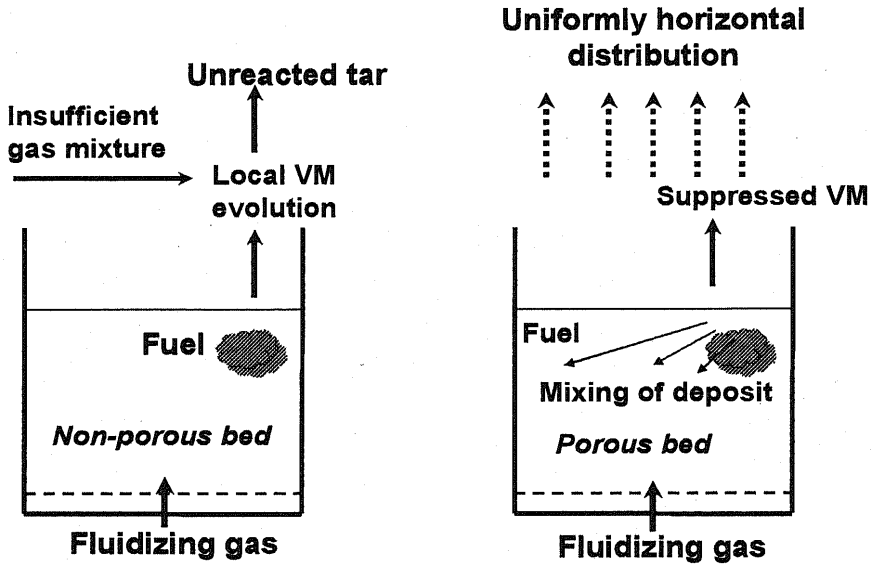

Fig. 1-6 Mechanism of the enhancement of horizontal dispersion of carbon deposited.

An innovation method is needed to measure horizontal dispersion of solids at high bed temperatures that resemble those of commercial operations. Carbon-loaded porous bed materials that had been prepared by capacitance effect (volatile matter capture by porous particles) have a possibility to use as a tracer.

Quantitative analyses incorporating the combustion rate of carbon deposits, the solid dispersion rate, and the horizontal scale of combustor are necessary to apply porous bed materials to large-scale combustors. In addition, for rational scaling-up of reactors, the removal rate of carbon deposits must necessarily be raised, but

information to do so is still lacking. Therefore, it is necessary to establish a model of a bubbling fluidized bed combustor (BFBC) in which both carbon deposit combustion and horizontal solid dispersion occur simultaneously.

1.6 Content of the present thesis

The overview of this thesis is divided into three objective studies in the following way within five chapters as bellows:

Chapter 1: General introduction

Chapter 2: Reduction of volatile matter evolution rate from a plastic pellet during bubbling fluidized bed pyrolysis by using porous bed material

Chapter 3: A new method to evaluate horizontal solid dispersion in a bubbling fluidized bed.

Chapter 4: Model of combustion and dispersion of carbon deposited on porous bed material during bubbling fluidized bed combustion

Chapter 5: Conclusion

The first study deals with reduction of VM evolution of wastes fuels. The contribution of reduced heat transfer rate and capacitance effect to the delay of volatile matter evolution is evaluated by employing various bed materials with and without capacitance effect.

The second study is proposed to develop a new method to evaluate horizontal dispersion of solids in bubbling fluidized beds. A carbon-loaded bed material prepared using the capacitance effect (volatile matter captured by porous particles) is used as a tracer. Two carbon-solid tracers were prepared: using a carbon-loaded bed material with dividing bed using a partition plate, and using activated carbon batch injection. A comparison is also made with the literature results.

The third objective deals with a mathematical model which includes carbon deposited combustion and horizontal dispersion. In this study, the oxidation rate of carbon deposits is measured by burning carbon deposits with oxygen and measuring the produced CO_2. Based on the burning rate of carbon deposits, a one-dimensional mathematical model of carbon deposit combustion in a bubbling fluidized bed is developed. A two-dimensional mathematical model to predict the horizontal concentration profile of carbon combustion is also developed by taking account of both the reaction rate and solid dispersion. Experiments using a two-dimensional bubbling fluidized bed validated the model.

7. References

1. K. Sandelin, B. Coda, R. Backman, R . Berer, K.R.G Hein, Melting of ash components when co-firing coal, straw and paper sludge under BFB conditions. In: Donald W, Geiling PE, editor. 16th International Conference on FBC. New York, USA: ASME; 2001. FBC01-0129.
2. J.L. Easterly, M. Burnham, Overview of biomass and waste fuel resources for power production. Biomass Bioenergy 1996;10:79–92.
3. J. Werther, M. Saenger, E. Hartge, T. Ogada, Z. Siagi , Combustion of agricultural residues. Progress in Energy and Combustion Science 2000;26(1):1-27.
4. E. Natarajan, A. Nordin, A.N. Rao, Overview of combustion and gasification of rice husk in fluidized bed reactors. Biomass and Bioenergy 1998;14(5-6):533-546.
5. N. Kiran, E. Ekinc and C. E. Snape, Recyling of plastic wastes via pyrolysis Resources. Conservation and Recycling 2000;29(4):273-283.
6. A. Demirbas, Pyrolysis of municipal plastic wastes for recovery of gasoline-range hydrocarbons. Journal of Analytical and Applied Pyrolysis 2004;72(1):97-102.
7. A. G. Buekens, H. Huang, Catalytic plastics cracking for recovery of gasoline-range hydrocarbons from municipal plastic wastes Resources. Conservation and Recycling 1998 23;3;163-181.

8. T. Ogada, J .Werther, Combustion characteristics of wet sludge in a fluidized bed: release and combustion of the volatiles. Fuel 1996;75:617–626.

9. J.S. Chern, N. A.Hayhurst, Does a large coal particle in a hot fluidised bed lose its volatile content according to the shrinking core model? Combustion and Flame 2004 139 (3) 208-221.

10. F. Scala, R.Chirone, Fluidized bed combustion of alternative solid fuels. Experimental Thermal and Fluid Science 2004;28(7) 691-699.

11. N. Fujiwara, M. Yamamoto, T. Oku, K. Fujiwara, S. Ishii, CO reduction by mild fluidization for municipal waste incinerator. In: Proc. of 1st SCEJ Symposium on Fluidization. Tokyo, Japan: SCEJ; 1995.p.51-5.

12. K. Koyama, M. Suyari, F. Suzuki, M. Nakajima, Combustion technology of municipal fluidized bed technology. In: Proc. of 1st SCEJ Symposium on Fluidization. Tokyo, Japan: SCEJ; 1995.p.56-63.

13. T. Izumiya, K. Baba, J. Uetani, H. Hiura, M. Furuta, Experimental study of combustion and gas flow at freeboard of fluidized combustion chamber for municipal waste. In: Proc. of 3rd SCEJ Symposium on Fluidization. Nagoya, Japan: SCEJ; 1997.p.210-5.

14. H.J. Franke, T. Shimizu, A. Nishio, H. Nishikawa, M. Inagaki, W. Ibashi, Improvement of carbon burn-up during fluidized bed incineration of plastic by

using porous bed materials. Energy & Fuels 1999;13:773-7.

15. H.J. Franke, T. Shimizu, S.Hori, Y. Takano, M. Tonsho, M. Inagaki, M.Tanaka, Simultaneous reduction of NOx emission and unburnt hydrocarbon emission during plastic incineration in fluidized bed combustor. In: Donald W, Geiling PE, editor. 16th International Conference on FBC. New York, USA: ASME; 2001.FBC2001-94.

16. T. Shimizu, H.J. Franke, S. Hori, Y. Takano, M. Tonsho, M. Inagaki, M. Tanaka, Porous bed material – An approach to reduce both unburnt gas emission and NOx emission from a bubbling fluidized bed waste incinerator. Journal Japan Inst. Energy 2001;80:333-42.

17. T. Shimizu, H.J. Franke, S. Hori, T. Yasuo, K. Yamagiwa, M. Tanaka, In-situ hydrocarbon capture and reduction of emissions of dioxins by porous bed material under fluidized bed incineration conditions. In: Pitsupati S, editor. 17th International Conference on FBC, Jacksonville FL, USA: ASME; 2003.FBC2003-031.

18. T. Namioka, K. Yoshikawa, H. Hatano, Y. Suzuki, High tar reduction with porous particles for low temperature biomass gasification: Effects of porous particles on tar and gas yields during sawdust pyrolysis. J. Chem. Eng. Japan 2003;36:1440-8.

19. K. Ito, Moritomi H, Yoshiie R, Uemiya S, Nishimura M. Tar capture effect of porous particles for biomass fuel under pyrolysis conditions. J. Chem. Eng. Japan 2003;36:840-5.

20. G. Piao, S. Aono, K. Motohiro, R. Yamazaki, S. Mori. Combustion test of refuse derived fuel in a fluidized bed. Waste Management 2000;20(5-6) 443-447.

21. Hosada H., Hirama T., ,A novel technique for simultaneous reduction of nitrous and nitrogen oxides emissions from a FBC combustor. In Proceeding of the International Conference on FBC 14th, 1995 pp. 1469 – 1475.

22. Lyngfel A., Amand L-E, Leckner B., Reversed air staging- a method for reduction N2O emission from fluidized bed combustion of coal. Fuel 1998;77: 953-969.

23. T. Miyauchi,. T. Tsutsui, Y. Nozaki, A new fluid thermal cracking process for upgrading residues, paper presented at the AIChE National Meeting (Houston, Texas) 1987.

24. H.J. Franke, T. Shimizu, S. Hori, Y. Takano、M. Tonsho, M. Inagaki, M. Tanaka, Simultaneous reduction of Nox emission and unburnt hydrocarbon emission during plastic incineration in FBC. In: 16th International Conference of FBC 2001; paper no.94.

25. 7. T. Shimizu, H.J. Franke, S. Hori, T. Yasuo, K. Yamagiwa, M. Tanaka, In-situ

hydrocarbon capture and reduction of emissions of dioxins by porous bed material under fluidized bed incineration conditions. In: Pitsupati S, editor. 17th International Conference on FBC, Jacksonville FL, USA: ASME; 2003.FBC2003-031.

26. T. Shimizu, T. Nemoto, H. Tsuboi, T. Shimoda, S. Ueno. Rice husk combustin in A FBC using porous bed material. In 18th International Conference of FBC, Toronto 2005, paper No. FBC2005-78028.

27. H.J. Franke, T. Shimizu, S. Hori S, Y. Takano, M. Tonsho, M. Inagaki, M. Tanaka, Suppression of rapid devolatilization of plastic during bubbling fluidized bed combustion using porous bed material. In: 3rd European Conference on Fluidization. Toulouse, France; 2000.p.641-8.

28 H.J. Franke, T. Shimizu, S. Hori, Y. Takano, M. Tonsho, M. Inagaki, M. Tanaka, Reduction of devolatization rate of fuel during bubbling fluidized bed combustion by use of porous bed material. Chemical Engineering and Technology 2001;24(7):725-33.

Chapter 2

Reduction of volatile matter evolution rate from a plastic pellet during bubbling fluidized bed pyrolysis by using porous bed material

2.1 Introduction

Fluidized Bed Combustors (FBCs) using biomass and wastes as fuels for power generation is recognized to have benefits such as recovering the large amounts of energy remaining in the fuels, reducing the waste volumes, etc. One feature of biomass and wastes as fuels is high volatile matter content. Due to high heat transfer from the bed material to fuel, volatile matter evolution occurs very rapidly when fuel is fed into the bed. Thus local volatile matter evolution takes place only in the vicinity of the fuel feed point. If the mixing of gas in the upper freeboard is insufficient in fluidized bed combustors, complete combustion is not easy. Often unburned hydrocarbons are released from combustors and it is anticipated that dioxins are formed from such unburned hydrocarbons (PCDDs and PCDFs) [1, 2]. Another problem of local volatile matter evolution is local heat release in the freeboard, which forms locally high temperature region and enhances NOx formation.

Numerous investigations have been conducted to minimize the formation of harmful dioxins caused by the high rate of volatile matter evolution. Reducing bed temperature and reducing gas superficial velocity into the bed lead to lower heating rate during waste combustion [3]. Controlling the waste feed rate suppresses the fluctuation of volatile matter evolution [4], and introducing baffles in the freeboard enabled to enhance the mixing of air to volatile matter [5].

Another possible measure to suppress the rapid volatile matter evolution is the use of porous bed material that captures hydrocarbon in the pores as carbon deposit, so called "capacitance effect" [6 - 11]. It reduces the amount of evolved volatile matter and increases the conversion of carbon in the dense bed, thus it is expected to enhance the horizontal dispersion of carbonaceous materials and to inhibit the formation of local fuel-rich zone as well as high temperature zone in the freeboard [6 - 8]. Another advantage of porous bed material is lower heat transfer rate from bed to the fuel. Porous bed material was reported to reduce heat transfer rate, thus it delayed volatile matter evolution [7, 12, 13]. However, the previous works were conducted using porous solids with capacitance effect. Thus it is possible that the former results of delayed volatile mater evolution were affected by both reduced heat transfer and by capacitance effect. The effect of solely heat transfer rate on volatile matter evolution rate has not yet been fully clarified.

In this work, porous solids which have capacitance effect and negligible capacitance effect were employed as bed materials. Heat transfer rate, volatile capture, and volatile matter evolution rate were measured. The relative importance heat transfer and capacitance effect on volatile matter evolution is discussed.

2.2 Experimental

2.2.1 Measurement of devolatilization rate and volatile matter capture

Devolatilization experiments were conducted using a laboratory-scale bubbling fluidized bed reactor of 5.3 cm in inner diameter, as shown in Fig. 2-1.

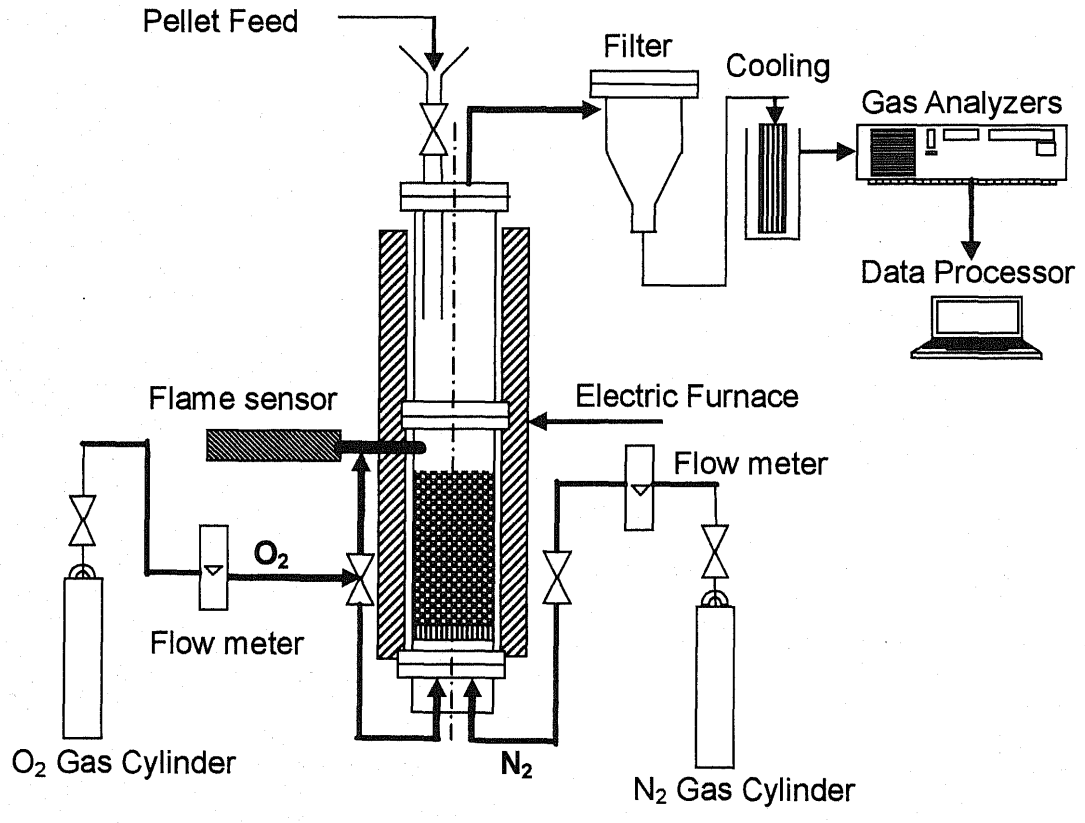

Fig. 2-1. Fluidized bed apparatus for devolatilization.

The bed was heated up electrically and the bed temperature was maintained at 943K. Four types of porous bed materials, porous silica Q6, porous alumina MSC, MS-1B and AB were employed. For AB, two different size fractions were employed. The properties of porous bed materials are shown in Tab. 1. Porous materials MSC, MS1-B and AB had capacitance effect whereas Q6 made from highly pure silica did not capture volatile matter as shown later. Also non-porous bed quartz sand (QS) of 273 μm was employed for comparison. The bed material was packed in the reactor with a static bed height of 10 cm. The bed was fluidized by nitrogen gas at superficial velocities of 0.13 m/s and 0.21 m/s. A detector of ultraviolet light (UV), which is formed during flame combustion, with an oxygen injection nozzle was installed in the freeboard at 25 cm above the distributor.

Table 2-1. Properties of porous particles.

Composition[wt%]	MS-1B	MSC	AB		Q6
Al_2O_3	84.7	93.7	69.4		-
SiO_2	2.2	-	7.2		100
TiO_2	1.1	-	13.0		-
Fe_2O_3	5.8	0.3	8.4		-
CaO	0.8	-	0.3		-
SO_3	3.8	1.9	0.8		-
size[μm]	399	200	Coarse AB	Fine AB	253
			385	237	
A* [m^2/g]	195	211	124		450
V** [cm^3/g]	0.32	0.45	0.20		0.89

* A: surface area, **V : pore volume.

To simulate high volatile fuel, cylindrical polyethylene pellets were used with typical size of 1cm in diameter and 1 cm in length. A fuel pellet was fed from the top of the reactor onto the dense bed. After the fuel feed, heat up and devolatilization took place. The upward streaming volatile matter was mixed with oxygen supplied through the oxygen nozzle, and it was burned. During flame combustion, ultraviolet light emission was detected by the UV-sensor, thus the time for the devolatilization was measured. After devolatilization, the amount of captured carbon was determined by feeding oxygen into the bed to burn it and measuring the concentration of CO_2 in the flue gas. Flue gas was sampled at the reactor exit after removing particles with a silica filter and removing water vapor by cooling in an ice bath. Concentrations of O_2 were measured by paramagnetic continues gas analyzer. Concentrations of CO and CO_2 were measured by NDIR analyzers.

There are two approaches to determine the onset of devolatilization as an index of devolatilization rate. One is the detection of gaseous products such as CO_2 and CO, both of which are formed by the oxidation of the volatile matter with oxygen injected into the freeboard. The other is the detection of flame combustion of volatile matter by detecting UV light. The response of the former is usually slower than the latter due to the time lag in the gas sampling line and the infrared absorption chamber in the NDIR analyzer. The detection of UV light is sufficiently fast since it

detects the light formed in the reactor without any time lag, provided the flame is formed. However, if the concentration of volatile matter is too low to maintain the flame, the detection of UV light may fail to detect volatile matter evolution. If the capacitance effect is too strong, such failure may occur. In this work both approaches, detection of gaseous products and UV light, were employed. For the detection of gaseous products, the time lag due to the delay of the analyzer was corrected by measuring the delay using impulse injection of standard gas.

2.2.2 Heat Transfer Measurement

The experiments were carried out in a fluidized bed reactor made of stainless steel with inner diameter of 53 mm. The reactor was covered with electric heating elements to control the bed temperature. The bed temperature was 943K. In order to avoid the corrosion of the probe surface, nitrogen was employed as fluidizing gas. The gas velocities were 0.13 m/s, 0.17 m/s and 0.21 m/s. The same bed materials as the devolatilization experiments were employed. The same static bed height as the devolatilization experiments of 10 cm was employed.

A brass cylinder of 10 mm in diameter with 11.2 mm in length was used as a probe. The cylindrical shape was similar with the shape of the fuel pellets employed for the devolatilization experiments. Thermocouple wires (diameter, Φ = 0.32mm)

were lead to the center of the probe and there joint by a brass nail to form thermocouple (Fig. 2-2).

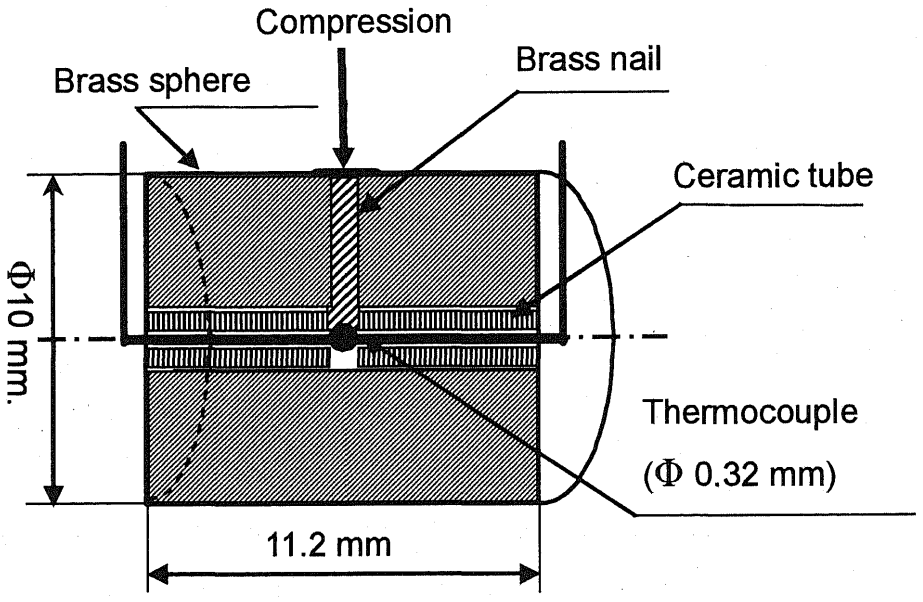

Fig. 2-2 Probe to measure heat transfer coefficient.

The bed was heated to a temperature of 943 K, and then the probe at a room temperature was fast dipped into the bed to a position 2 cm below the surface of the static bed until a constant probe temperature was reached. The temperature of the probe (T) and the bed temperature (T_b) were measured using the thermocouples and recorded in a computer. Assuming that the heat conduction in the probe was so good that the temperature in the probe was uniform, the change in the probe temperature can be written as follows:

$$C_{prob}\rho_{prob}V_{prob}\frac{dT}{dt} = hS_{prob}(T_b - T) \qquad (2\text{-}1)$$

where h is the heat transfer coefficient. With the known data for probe's density

(ρ_{prob}), probe's volume (v_{prob}), external surface area (S_{prob}) and specific heat (C_{prob}), heat transfer coefficient can be determined.

$$\frac{T(t)-T_b}{T(0)-T_b} = \exp\left(-\frac{hS_{prob}}{C_{prob}\rho_{prob}v_{prob}}t\right) \quad (2\text{-}2)$$

$$h = \frac{C_{prob}\rho_{prob}v_{prob}}{S_{prob}t}\ln\left(\frac{T(0)-T_b}{T(t)-T_b}\right) \quad (2\text{-}3)$$

2.3 Results and Discussion

2.3.1 Measurement of devolatilization rate and volatile matter capture

Typical results of the change in CO_2 concentration in the flue gas are shown in Fig. 2-3. Volatile matter evolved after one plastic pellet was fed into the dense bed. The volatile matter that escaped from the bed was then burned in the freeboard by injecting O_2 through the UV-detector nozzle and the produced CO_2 was measured. Then oxygen was fed into the dense bed to burn carbon deposit. For porous silica Q6, negligible amount of CO_2 was detected during carbon deposit combustion. This indicates that the polyethylene pellet was all converted to volatile matter and the volatile matter was not captured by Q6. Porous bed Q6 had no capacitant effect though the internal surface area was the largest among the samples.

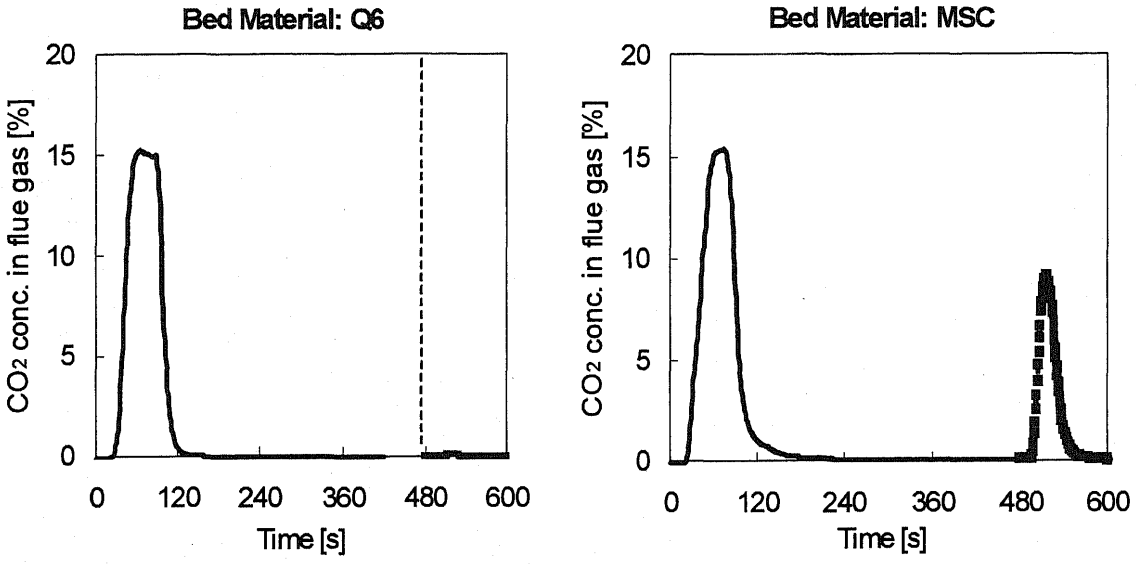

Fig. 2-3 Carbon deposit formation over bed materials (time 0 - 480 s: volatile matter evolution followed by its combustion in the freeboard by feeding oxygen through the UV-detector nozzle; time 480 – 600 s: combustion of carbon deposit by feeding oxygen into the bed.

In contrary, when porous alumina MSC was employed in the bed, a significant production of carbon dioxide was detected during oxygen feed to the dense bed. This indicates that MSC captured volatile matter form the pellet, i.e. MSC has capacitant effect.

Fig. 2-4 shows the effect of solid type and gas velocity on volatile matter capture. The volatile matter capture efficiency was defined as the amount of carbon deposit divided by the amount of carbon in the fuel pellet, since the fuel (polyethylene pellet) was converted completely to the volatile matter without forming char (Fig. 2-3a). Four types of porous bed materials were employed at given superficial gas

velocities of 0.13 m/s and 0.21 m/s. Porous silica Q6 had negligible activity to capture carbon in the volatile matter. Other porous bed materials, MSC, MS-1B, fine and coarse AB, captured volatile matter significantly. Especially, fine AB had high activity and captured approximately 30 % of volatile matter at lower gas velocity (13 cm/s), though the carbon capture was reduced to 20 % at higher gas velocity. MSC, MS-1B, and coarse AB captured approximately 20 % of volatile matter.

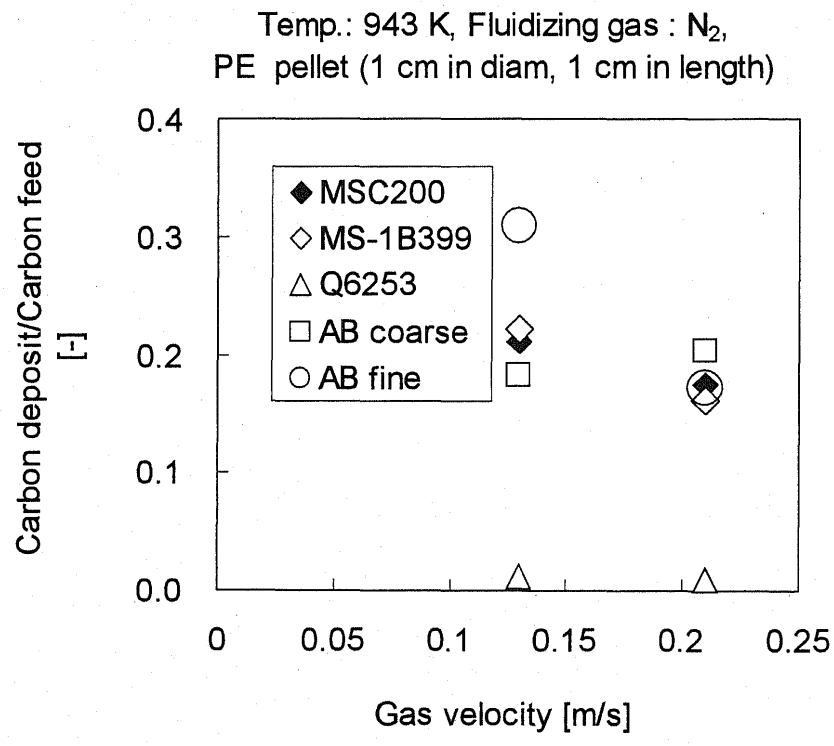

Fig. 2-4. Effect of gas velocity on carbon deposit/carbon feed.

Fig. 2-5 shows the typical output signals of UV detector during combustion of volatile matter released from a polyethylene pellet at a gas velocity of 0.13 m/s. For QS, flame combustion started soon just 8 s after the pellet was fed. It then was followed by Q6 at 16s, coarse AB at 21s and the last one was MS-1B at 30s. As an

index of volatile matter evolution rate, the onset of flame detection by the UV detector was chosen in this work in the same manner as previous work [13].

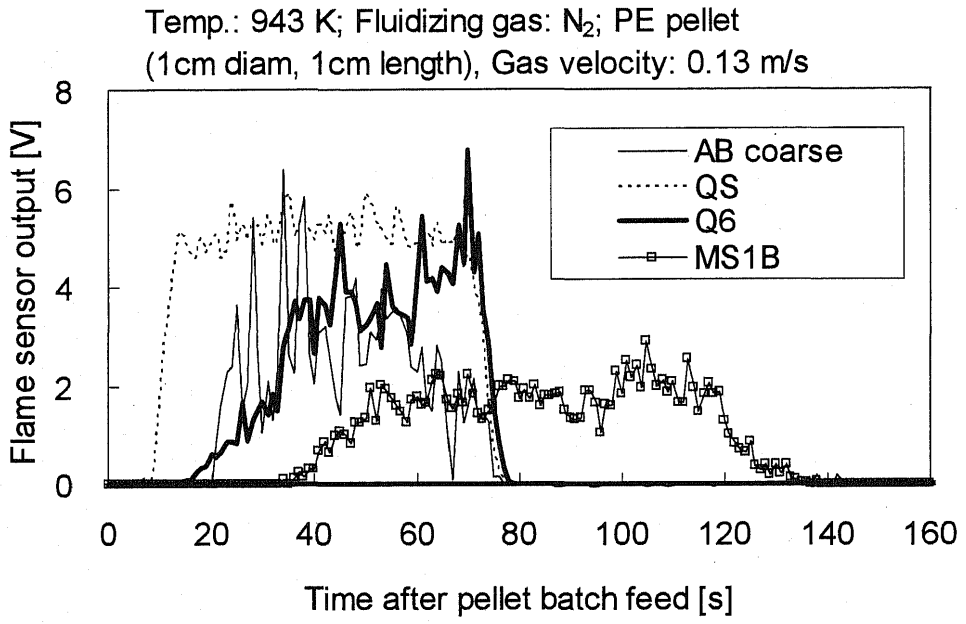

Fig. 2-5. Typical output signal from UV detector during devolatilization.

The onset of flame detection in relation to capture carbon for different bed materials is shown in Fig. 2.6. At a velocity of 0.13 m/s, the volatile matter capture was almost the same among MSC, MS-1B and coarser AB (AB385), but the onset of flame detection was totally different among them. Finer AB (AB237) had the highest volatile matter capture and it showed the latest onset of devolatilization. Although Q6 had negligible capacitance effect, the onset of flame detection was between MSC and coarser AB (AB385). Thus it can be concluded that the onset of the devolatilization had no clear relationship with the capacitance effect.

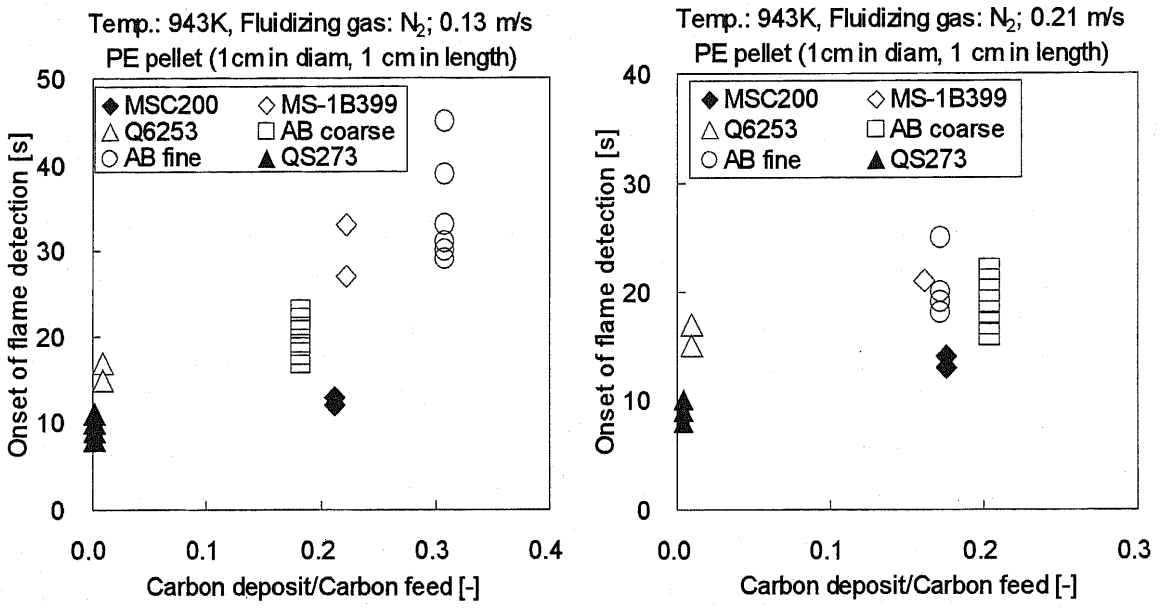

Fig. 2-6. Onset of flame detection vs. carbon deposit on different bed materials.

2.3.2 Heat transfer coefficient

Fig. 2-7 shows the transient change difference in the temperature between the fluidized bed and the probe. Since $\ln(T - T_b)$ had straight-line relationship with time, average heat transfer coefficients were calculated from the slope in Fig. 2-8 according to eq. 2-3. Fig. 2-8 shows the effect of gas velocity on the heat transfer coefficient. The heat transfer coefficient for porous alumina MSC, MS-1B, and AB (both coarse and fine) increased slightly with increasing gas velocity, while it was almost constant for porous silica Q6. Comparison was made with non-porous bed material quartz sand (QS273), which had the highest heat transfer coefficient and also had a tendency to increase slightly with increase in gas velocity. For porous bed material AB, this figure also indicates that the smaller fraction (AB237) had

higher heat transfer coefficient than the coarser fraction (AB385). Usually, the heat transfer coefficient of smaller particles is larger than that of coarser particles [14]. Nevertheless, the heat transfer coefficient of QS (273 μm) was higher than those of MSC (200 μm), fine AB (237 μm) and Q6 (253 μm) in spite of larger size.

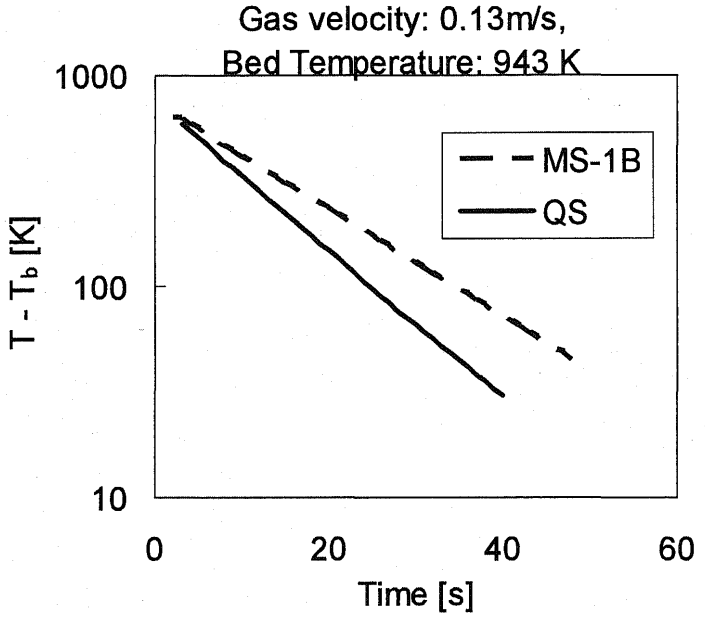

Fig. 2-7. Transient change in the difference in temperature between heat transfer probe and fluidized bed after dipping probe into hot fluidized bed (measurement of heat transfer coefficient at gas velocity = 0.13 m/s).

This is attributable to the lower density of particles. According to the packet renewal model proposed by Mickley and Fairbanks [15, 16], heat transfer coefficient is given from thermal conductivity of emulsion (k_e^o), particle density (ρ_s), void fraction in the emulsion (ε_{mf}), specific heat of particle (C_{ps}), bubble frequency (n_w), and the bubble fraction in the bed (δ_w).

$$h = 1.13\left[k_e^{\circ}\rho_s(1-\varepsilon_{mf})C_{ps}n_W/(1-\delta_w)\right]^{1/2} \quad (2\text{-}5)$$

Since porous particles have lower particle density than non-porous sand, they could suppress the heat transfer rate.

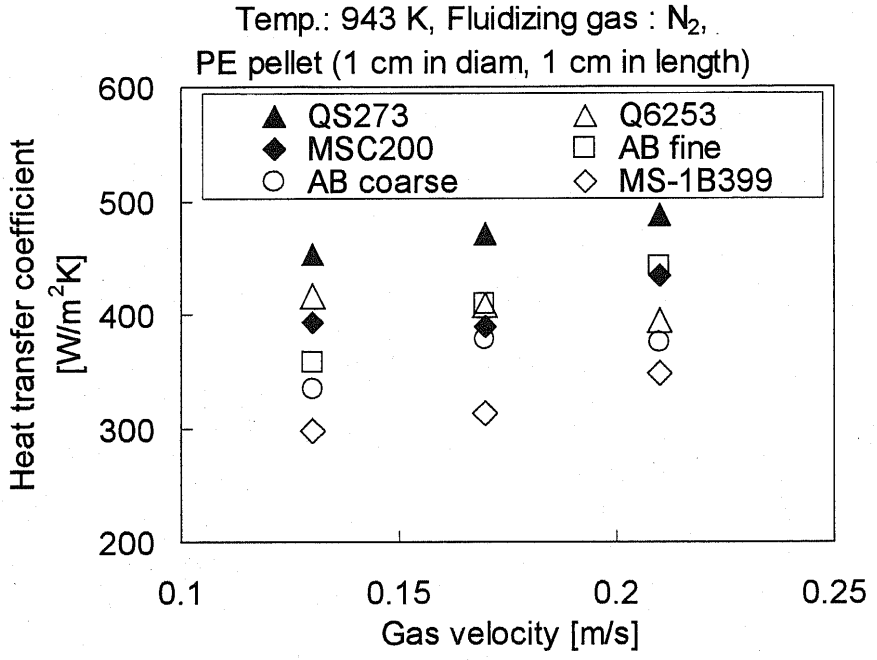

Fig. 2-8. Effect of gas velocity and porous bed type on heat transfer coefficient.

Fig. 2-9 shows the relationship between heat transfer coefficient and the onset of flame detection by the UV detector. The onset of the flame detection was well correlated with the heat transfer coefficient among QS, MSC, Q6, coarse AB (AB385) and MS-1B. However, when fine AB (AB237) was employed as a bed material, the flame combustion was detected later in spite of relatively high heat transfer coefficient, comparing to the relationship observed for other solids. An explanation of the delay of flame combustion is the highest capacitance effect of fine AB; the volatile matter capture efficiency for fine AB was about 0.3 whereas it

was at best 0.2 for other solids. Due to high volatile matter capture by the fine AB, the concentration of volatile matter in the freeboard could not be sufficient to maintain flame combustion, thus the onset of the flame detection was delayed.

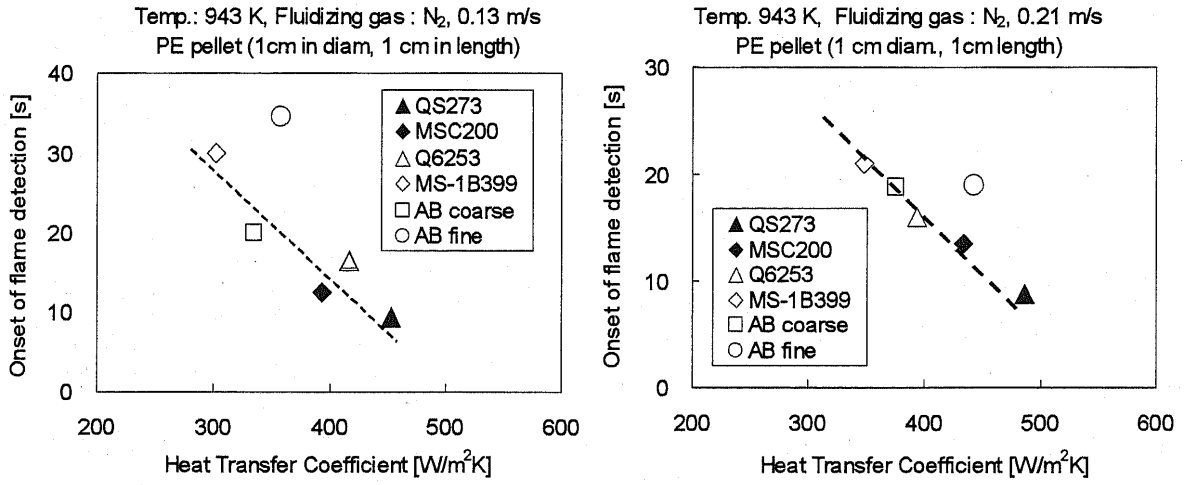

Fig. 2-9. Relationship between the onset of flame detection and heat transfer coefficient for different gas velocities.

Fig. 2-10 shows the relationship between the onset of flame detection and onset of CO_2 detection for different gas velocity of 0.13 m/s and 0.21 m/s. Except for fine AB, the onset of flame detection agreed well with the onset of CO_2 detection or flame detection occurred earlier than CO_2 detection. The delay of CO_2 detection may be due to the distance from the reactor to the gas analyzer unit. When fine AB was employed, the onset of flame detection was considerably later than the onset of CO_2 detection, especially at lower gas velocity (13 cm/s). This is attributable to the high of volatile matter capture efficiency of fine AB, consequently the concentration

of volatile matter was not sufficient to perform quick flame combustion. Instead, the onsets of emissions of CO and CO_2 from the reactor were observed earlier for the fine AB. Thus for solids with strong capacitance effect, detection of produced gaseous components is considered to be a better approach to detect the onset of devolatilization rather than the detection of flame combustion, though the detection of flame combustion is better approach for solids moderate capacitance effect.

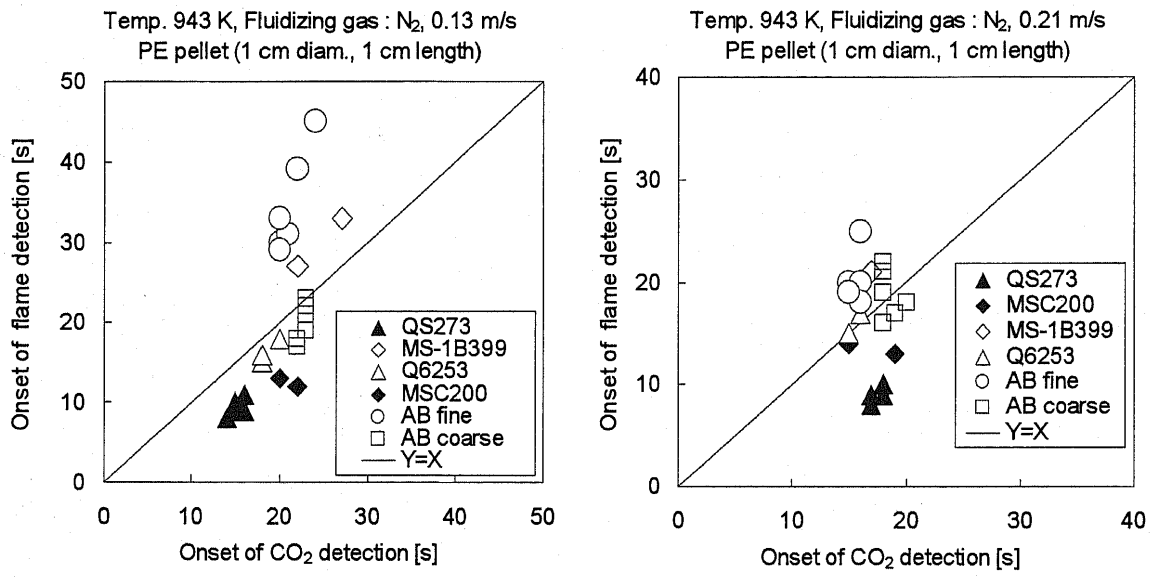

Fig. 2-10. Onset of flame detection vs. onset of CO_2 detection.

The minimum among the onset of flame combustion (t_{flame}), the onset of CO_2 detection (t_{CO2}) and the onset of CO detection (t_{CO}) to the average heat transfer coefficient is shown in Fig. 2.11. This figure shows that the onset of devolatilization was well correlated with the heat transfer coefficient for all type of bed materials. Comparison to Figs. 9 and 10 can give an explanation that the late of flame and CO_2 detection for fine AB was due to high efficiency of capacitant effect.

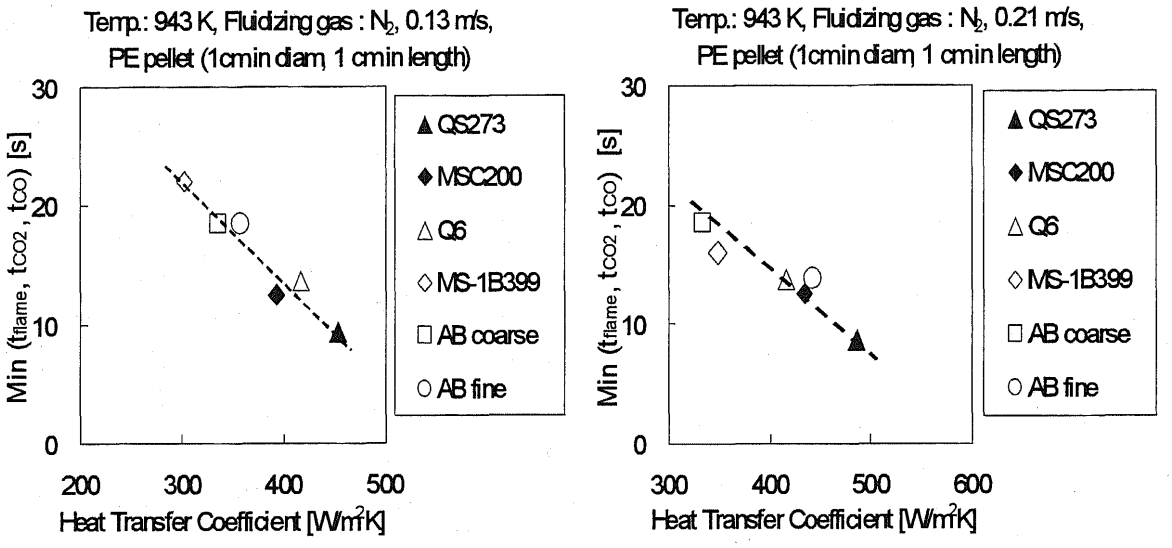

Fig. 2-11. Minimum among the onset of flame detection, the onset of CO_2 detection and the onset of CO detection vs. heat transfer coefficient.

2.4. Conclusions

Various porous bed materials were employed in fluidized bed experiments to evaluate the effect of volatile matter capture and heat transfer coefficient to the delay of devolatilization during heat up of plastic pellets. The onset of flame detection was found to be delayed by employing porous bed materials compared to non-porous quartz sand. Volatile matter capture (capacitance effect) and heat transfer coefficient of the porous solids were also measured. For four different types of porous bed, Q6, coarse AB, MSC and MS-1B, all of which had volatile matter efficiency lower than 0.2, the onset of flame detection was mainly determined by the heat transfer rate. However, the delay of the flame combustion for fine AB was observed, although this bed material had relatively high heat transfer coefficient.

This was due to the strong capacitance effect which reduced volatile matter concentration in the freeboard to form flame. For bed materials with strong capacitance effect, detection of gaseous components will be better approach, though the delay of the measurement apparatus should be corrected and the correction of the delay may cause the inaccuracy of measurement of time.

Symbols used

C_{prob}	[J/kgK]	specific heat of probe
C_{ps}	[J/kgK]	specific heat of particle
h	[W/m^{2}K]	heat transfer coefficient
k_e^o	[W/mK]	thermal conductivity of emulsion
n_w	[1/s]	bubble frequency
S_{probe}	[m^2]	external surface area of probe
T	[K]	temperature of probe
T_b	[K]	bed temperature
t	[s]	time
t_{CO}	[s]	the onset of CO detection
t_{CO2}	[s]	the onset of CO_2 detection
t_{flame}	[s]	the onset of flame combustion

v_{prob}	[m^3]	volume of probe

Greek symbols

δ_w	[-]	bubble fraction
ε_{mf}	[-]	void fraction in the emulsion
ρ_{prob}	[kg/m^3]	density of probe
ρ_s	[kg/m^3]	density of particle

References

1. T. Lippert, A. Wokaun, D. Lenoir, Environment Science Technology, 1991, 25, 1485.

2. L. Stieglitz, G. Zwick, J. Beck, H. Bautz, W. Roth, Carbonaceous particles in fly ash -a source for the de-novo-synthesis of organochlorocompounds. Chemosphere 1989;19:283-290.

3. N. Fujiwara, M. Yamamoto, T. Oku, K. Fujiwara, S. Ishii, CO reduction by mild fluidization for municipal waste incinerator. In: Proc. of 1st SCEJ Symposium on Fluidization. Tokyo, Japan: SCEJ; 1995.p.51-5.

4. K. Koyama, M. Suyari, F. Suzuki, M. Nakajima, Combustion technology of municipal fluidized bed technology. In: Proc. of 1st SCEJ Symposium on

Fluidization. Tokyo, Japan: SCEJ; 1995.p.56-63.

5. T. Izumiya, K. Baba, J. Uetani, H. Hiura, M. Furuta, Experimental study of combustion and gas flow at freeboard of fluidized combustion chamber for municipal waste. In: Proc. of 3rd SCEJ Symposium on Fluidization. Nagoya, Japan: SCEJ; 1997.p.210-5.

6. H.J. Franke, T. Shimizu, A. Nishio, H. Nishikawa, M. Inagaki, W. Ibashi, Improvement of carbon burn-up during fluidized bed incineration of plastic by using porous bed materials. Energy & Fuels 1999;13:773-7.

7. H.J. Franke, T. Shimizu, S.Hori, Y. Takano, M. Tonsho, M. Inagaki, M.Tanaka, Simultaneous reduction of NOx emission and unburnt hydrocarbon emission during plastic incineration in fluidized bed combustor. In: Donald W, Geiling PE, editor. 16th International Conference on FBC. New York, USA: ASME; 2001.FBC2001-94.

8. T. Shimizu, H.J. Franke, S. Hori, Y. Takano, M. Tonsho, M. Inagaki, M. Tanaka, Porous bed material – An approach to reduce both unburnt gas emission and NOx emission from a bubbling fluidized bed waste incinerator. Journal Japan Inst. Energy 2001;80:333-42.

9. T. Shimizu, H.J. Franke, S. Hori, T. Yasuo, K. Yamagiwa, M. Tanaka, In-situ hydrocarbon capture and reduction of emissions of dioxins by porous bed

material under fluidized bed incineration conditions. In: Pitsupati S, editor. 17th International Conference on FBC, Jacksonville FL, USA: ASME; 2003.FBC2003-031.

10. T. Namioka, K. Yoshikawa, H. Hatano, Y. Suzuki, High tar reduction with porous particles for low temperature biomass gasification: Effects of porous particles on tar and gas yields during sawdust pyrolysis. J. Chem. Eng. Japan 2003;36:1440-8.

11. K. Ito, Moritomi H, Yoshiie R, Uemiya S, Nishimura M. Tar capture effect of porous particles for biomass fuel under pyrolysis conditions. J. Chem. Eng. Japan 2003;36:840-5.

12. H.J. Franke, T. Shimizu, S. Hori, Y. Takano, M. Tonsho, M. Inagaki, M. Tanaka, Suppression of rapid devolatization of plastics during bubbling fluidized bed combustion by use of porous bed material. In: Proceeding of 3rd European Conference on Fluidization, Toulouse 2000.

13. H.J. Franke, T. Shimizu, S. Hori, Y. Takano, M. Tonsho, M. Inagaki, M. Tanaka, Reduction of devolatization rate of fuel during bubbling fluidized bed combustion by use of porous bed material. Chemical Engineering and Technology 2001;24 (7):725-733.

14. D. Kunii, O. Levenspiel, Fluidization Engineering (2nd Edition). Stoneham:

Butterworth-Heinemann; 1991.p.277.

15. H.S. Mickley and C.A. Fairbanks, Mechanism of heat transfer to fluidized beds. AIChE Journal 1955;1:374-384.

16. H.S. Mickley, C.A. Fairbanks, R. D. Hawthorn. In: Chem. Eng. Prog. Symp. Ser.,1961.

Chapter 3

A new method to evaluate horizontal solid dispersion in a bubbling fluidized bed

3.1 Introduction

Horizontal mixing of solids in fluidized bed conversion processes is one of important components for operation and design of commercial units. The conversion efficiency of the system will decrease because of poor contact of solids with gaseous reactants if the solids are not fully mixed horizontally. In addition, poor solid mixing might cause undesired temperature profiles as a result of localized reactions. Therefore, to ensure good solid mixing, understanding of horizontal solid mixing phenomena is necessary.

Some reports have described methods of measuring horizontal solid mixing in fluidized beds. The experimental techniques usually involve injection of tracer particles into the bed. The necessary properties of tracers are: safe material that is easily obtained, handled, and detected, with particle density and size that are identical, or at least similar, to the bed material; the particles must be easily removed from the bed material after mixing, and be applicable to experiments at elevated temperatures. Various tracers have been used. Salt particles have been used [1, 2], but they present difficulties of tracer removal after the experiments. For

that reason, repeated experiments are usually difficult. Another type of tracer is magnetic [3], but it necessitates separation of tracers from the bed material after a single run. Radioactive tracers [4] are not easily obtained and require special care for handling. Tracer techniques using image analysis to follow the phosphor tracers or colored tracers were also used to investigate solid mixing [5, 6, 7, 8, 9], but the phosphor/colored tracers should be separated from the bed material before repeating the experiments. Furthermore, image analyses might only give information for a solid mixing view in the bed surface or through a transparent wall, the latter of which might contain the effect of disturbance of solid movement by friction between the wall and solids. A thermal technique was also developed using preheated bed particles [10, 11], but this method might include the effect of convective heat transfer between solids or between gas and solids. Use of frozen CO_2 (dry ice, CO_2 snow) particles has also been proposed [12], but their solid property (solid density) is fixed (approximately 1.6×10^3 kg/m^3) and it is not easy to prepare solids with different densities.

A new method is needed to evaluate horizontal dispersion of solids at high bed temperatures that resemble those of commercial operations. In this study, carbon-loaded porous bed materials that had been prepared by capacitance effect (volatile matter capture by porous particles) [13, 14, 15, 16, 17, 18] were used as

tracers. The present proposed method is based on transient change in the horizontal CO concentration profile in the freeboard. The experimental results were compared with results from the literature.

3.2 Principle of the Proposed Tracer Method

Porous particles are known to capture hydrocarbons within pores to form carbon deposits at high temperatures, as illustrated in Fig. 3-1 [13, 14, 15, 16, 17, 18]. This effect is called *capacitance effect*. Because the produced carbon-loaded particles contain only a few percent of carbon by mass, the apparent density, and therefore the hydrodynamic property, of the carbon-loaded particles is almost identical to that of raw particles. When the carbon-loaded solids are exposed to CO_2 at high temperatures, the carbon forms CO as

$$C + CO_2 \rightarrow 2CO \,. \qquad (3\text{-}1)$$

Assuming that the CO emission rate from the carbon deposit is proportional to the amount of carbon in the solids, the amount of carbon in the bed material can be determined by measuring the CO concentration in the flue gas sampled in the freeboard. The above assumption is practically valid for evaluation of horizontal solid dispersion because the reaction rate of C with CO_2 is so slow that the change in carbon loading in the solid over time is negligible for several minutes during

measurement of horizontal solid dispersion.

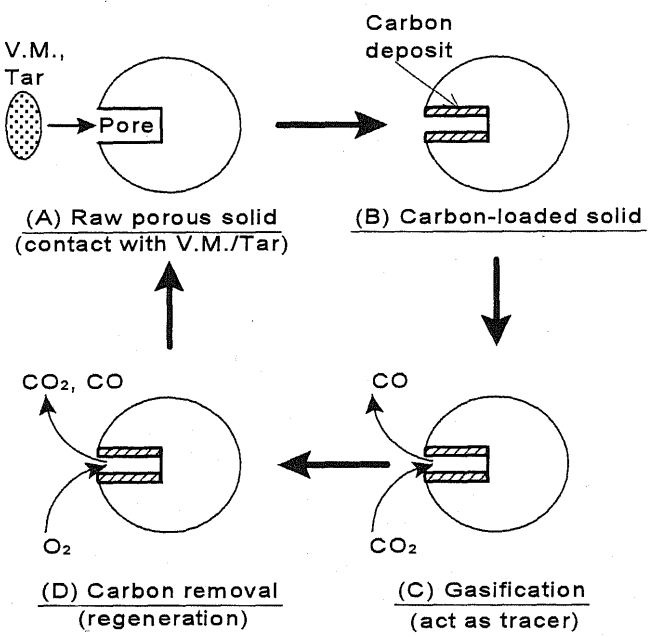

Fig. 3-1 Principle of this tracer method (carbon loading by capacitance effect, use of carbon-loaded solids as tracers, and regeneration of particles).

After the measurement of horizontal dispersion is finished, i.e., after uniform distribution of tracer particles throughout the bed is attained, the carbon can be removed by feeding oxygen (air) into the bed and burning carbon to regenerate raw porous particles. Then the measurement of horizontal dispersion coefficient is repeatable by feeding carbon-loaded particles into the bed.

3.3 Horizontal Dispersion of Bed Material in a Two-dimensional Bubbling Bed

In a two-dimensional bubbling fluidized bed, vertical mixing of solids is very good because of the vertical motion of bubbles, although horizontal solid dispersion is poor. Thereby, the solid dispersion can be treated as a one-dimensional diffusion

to the horizontal direction. One-dimensional diffusion of tracers is described using a partial differential equation as

$$D_h \frac{\partial^2 X(t,L)}{\partial L^2} = \frac{\partial X(t,L)}{\partial t} \quad , \tag{3-2}$$

where D_h is the horizontal dispersion coefficient [m^2/s]. The mass fraction of tracers in the bed material is $X(t, L)$, which is a function of position L [m] and time t [s]. The initial condition of eq. 3-2 is determined by the pattern of tracer injection; this will be given after describing the experimental procedure. This equation can be rewritten in a discrete form as

$$D_h \left\{ \frac{X(t,L+\Delta L)-2X(t,L)+X(t,L-\Delta L)}{(\Delta L)^2} \right\} = \frac{X(t+\Delta t,L)-X(t,L)}{\Delta t}, \tag{3-3}$$

where Δt and ΔL respectively denote the time step and distance between neighboring locations. When D_h has a relationship with Δt and ΔL of eq. 4, the transient change in X with a time step of Δt is given as eq. 3-5.

$$\frac{D_h \Delta t}{(\Delta L)^2} = \frac{1}{2} \tag{3-4}$$

$$X(t+\Delta t,L) = \frac{X(t,L+\Delta L)+X(t,L-\Delta L)}{2} \tag{3-5}$$

By solving eq. 3-5, the change in X with time is calculated numerically.

3.4 Experimental Apparatus and Procedure

3.4.1 Two-dimensional bubbling fluidized bed reactor

A laboratory-scale two-dimensional bubbling fluidized bed reactor with a cross

section of 0.16 m × 0.04 m and height above the distributor to the top of 0.71 m was used (Fig. 3-2). The bed was heated electrically and the bed was operated at 943 K and 1073 K. The bed material was porous alumina MS1B (particle size, 0.4 mm), whose properties are described elsewhere [16, 17, 18]. The static bed height was 0.10 m. The gas feed rate was 0.13 m/s. Four gas-sampling tubes were installed in the freeboard at distances from left wall of 0.02 m (probe #1), 0.06 m (probe #2), 0.10 m (probe #3), and 0.14 m (probe #4). The tube inlet height was 0.20 m. The gas samples from the sampling tubes were introduced to CO analyzers. The flue gas from the top of the reactor was also analyzed using a CO analyzer.

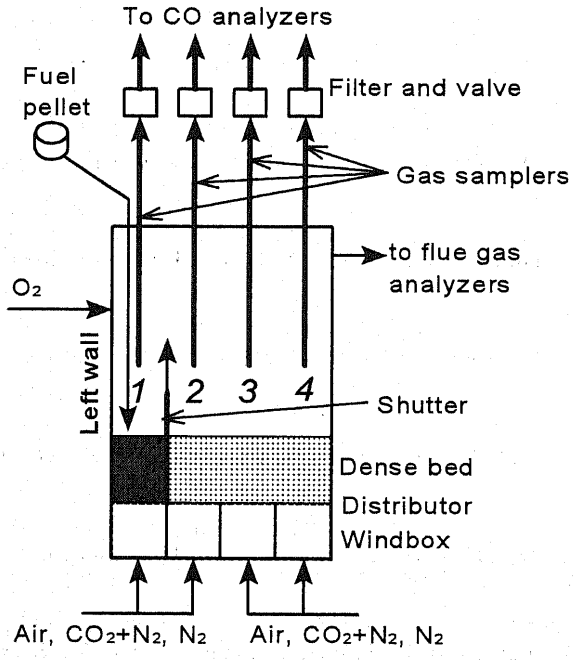

Fig. 3-2 Experimental apparatus for shutter method. Oxygen was injected into the freeboard only during devolatilization of PE pellets.

The dynamic response of the CO analyzer was identified by injecting an impulse of standard gas in the gas sampling line. The response of the analyzer could be

approximated by two completely-mixed vessels with time constants of 3.5 – 4.1 s connected in series.

3.4.2 Measurement of horizontal dispersion by tracers

3.4.2.1 Shutter method using carbon-loaded tracer

The fluidized bed was divided into two zones by a shutter (partition plate) located at 0.04 m from the left wall ($L_{shutter}$ = 0.04); then solid mixing after opening shutter was measured. First, the whole bed was fluidized using a N_2 stream and closing the shutter. Cylindrical polyethylene (PE) pellets with typical diameter of 1 cm and 1 cm length were fed into one side (left side in Fig. 3-2). During devolatilization of PE pellets, some of the volatile matter was captured by the bed material; thereby tracer particles (carbon-loaded particles) were prepared. Polyethylene is known to be converted to 100% volatile matter without forming char [16]. Therefore, the carbon in the bed material after devolatilization is considered to be carbon deposits within the pores. The carbon content in the tracer calculated from the total amount of PE pellets (approximately 6 g) and capture efficiency of 0.3 [16] was only 4%. Then the bed was fluidized using a mixture of CO_2 (15%) and N_2 (85%) to start carbon gasification. After CO evolution rate is stabilized, the shutter was opened by pulling it upward, thereby initiating solid mixing. During solid mixing,

the horizontal concentration profile of CO was measured continuously. After attaining complete mixing, the gas was switched to air to remove carbon by burning. The initial condition of the one-dimensional solid dispersion model (eq. 3-2) for the present shutter method is

$$X(0, L) = X_{init} \qquad \text{for } 0 < L < L_{shutter}, \text{ and} \tag{3-6}$$

$$X(0, L) = 0 \qquad \text{for } L_{shutter} < L. \tag{3-7}$$

3.4.2.2 Batch injection of tracer

In addition to the shutter method, batch injection of tracers at L_{batch} = 0.04 m was also conducted for comparison. As tracers, however, activated carbon particles with high reactivity (Tsurumi-coal 4GM; Tsurumi Coal Co. Ltd., size of 0.42–0.84 mm) were used because the gasification rate of the present carbon deposit, i.e., the CO evolution rate, was too low to measure the concentration accurately. Batch injection of tracers increases the total amount of solids in the reactor; it might affect the solid dispersion behavior. In addition, the time required for injecting a batch of solid will increase with increasing solid amount. Therefore, the batch amount must be limited. Consequently, highly reactive activated carbon particles were used. The initial condition for the batch injection is given as

$$X(0, L) = \delta(L_{batch}) , \tag{3-8}$$

where δ is Dirac's unit impulse function.

3.4.3 Effect of horizontal gas mixing

The horizontal concentration profile of CO released from the tracer particles is affected by not only solid dispersion but also horizontal gas mixing, thus effect of horizontal gas mixing in the bed and freeboard should be taken into consideration. The horizontal gas mixing was evaluated by using pure CO_2 as a tracer gas. The CO_2 gas was injected at different vertical positions (0.00, 0.05 and 0.10 m above the distributor) and horizontal positions (0.02, 0.06 and 0.08 m from the left wall). The sample gas from each probe was collected in a gas bag then analyzed using a gas chromatography. As reported previously [17], the vertical injection position had only minor influence on the horizontal concentration profile of the tracer gas, thus the dispersion is considered to take place mainly in the freeboard between bed surface and probe. In the following section, the theoretical concentration profile of the gas includes both effects of gas dispersion and the response of gas analyzer.

3.5 Results and Discussion

3.5.1 Shutter method using carbon-loaded tracer

Typical experimental results are presented in Fig. 3-3 to show the transient

change in CO concentrations in the gas samples taken by probe #1 at two different bed temperatures (943 K and 1073 K) after removal of the partition plate. Before opening the shutter, the bed beneath probe #1 was filled with tracer. Therefore, the CO concentration was the highest. The CO evolution rate dropped with the solid dispersion in the horizontal direction. To determine the dispersion coefficient, a comparison was made with the theoretical calculations using the one-dimensional diffusion model. By giving a value of D_h = 0.0003 m^2/s, the experimental results agreed with the diffusion model. They showed that the dispersion coefficient at the same gas feed rate was independent of temperature.

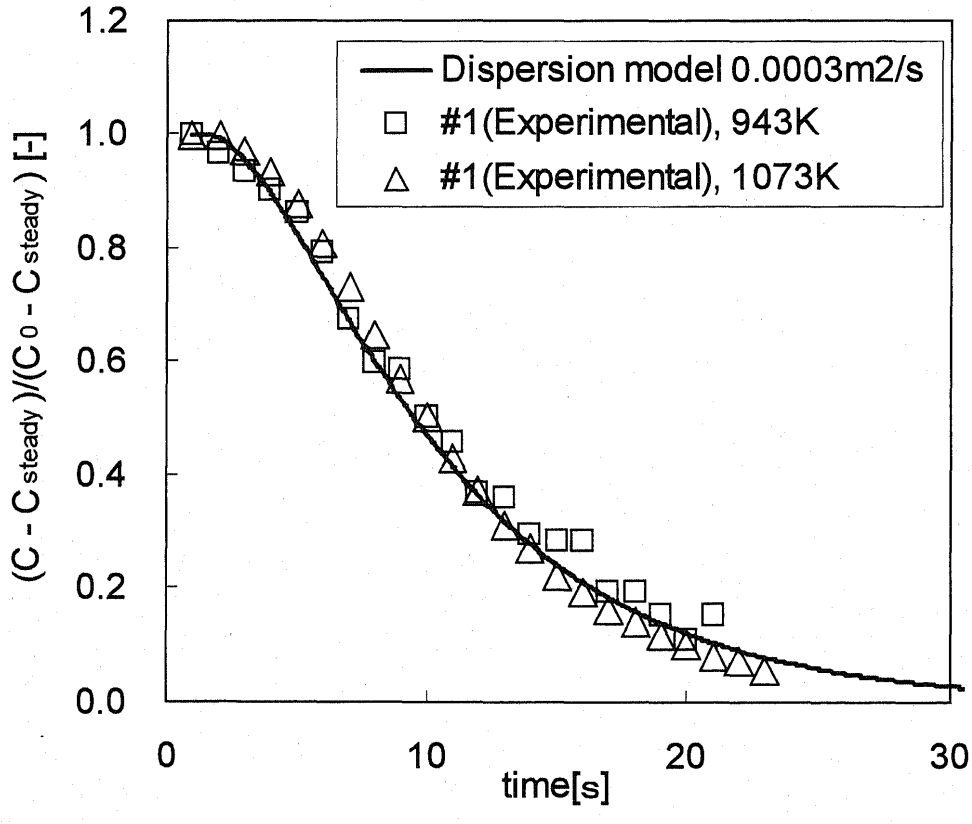

Fig. 3-3 Transient change in CO concentration for probe #1 after removing the shutter.

Figure 3-4 shows the transient change in CO concentration in the sample gas taken from probes #2, #3, and #4. Each result exhibits a different transient change, which is dependent on the distance from the tracer reservoir side (left side of the shutter in Fig. 3-2). The slowest response was found for #4, which is furthest from the tracer reservoir. The concentration increased at the beginning and became steady after attaining complete solid mixing. The present one-dimensional diffusion model with a value of D_h = 0.0003 m^2/s agreed with the experimental results similarly to results for probe #1.

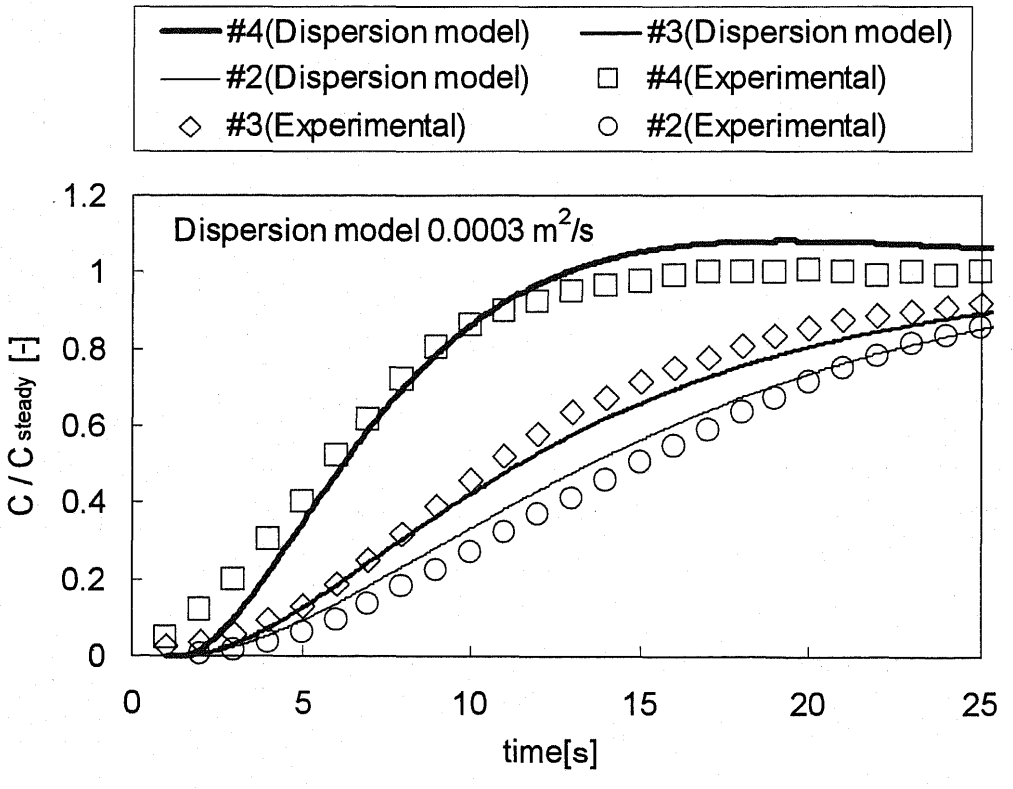

Fig. 3-4 Transient change in CO concentration for probes #2, #3, and #4 after removing the shutter.

3.5.2 Batch injection of activated carbon

Investigation was also made using batch injection of highly reactive activated carbon for comparison. The typical transient change in CO concentration is shown in Fig. 3-5. In this figure, the CO concentration is normalized by the concentration after attaining a steady state. A horizontal dispersion coefficient of 0.0002 m^2/s was found to match the experimental results. The present batch injection method gives a similar value of D_h to the value obtained using the shutter method.

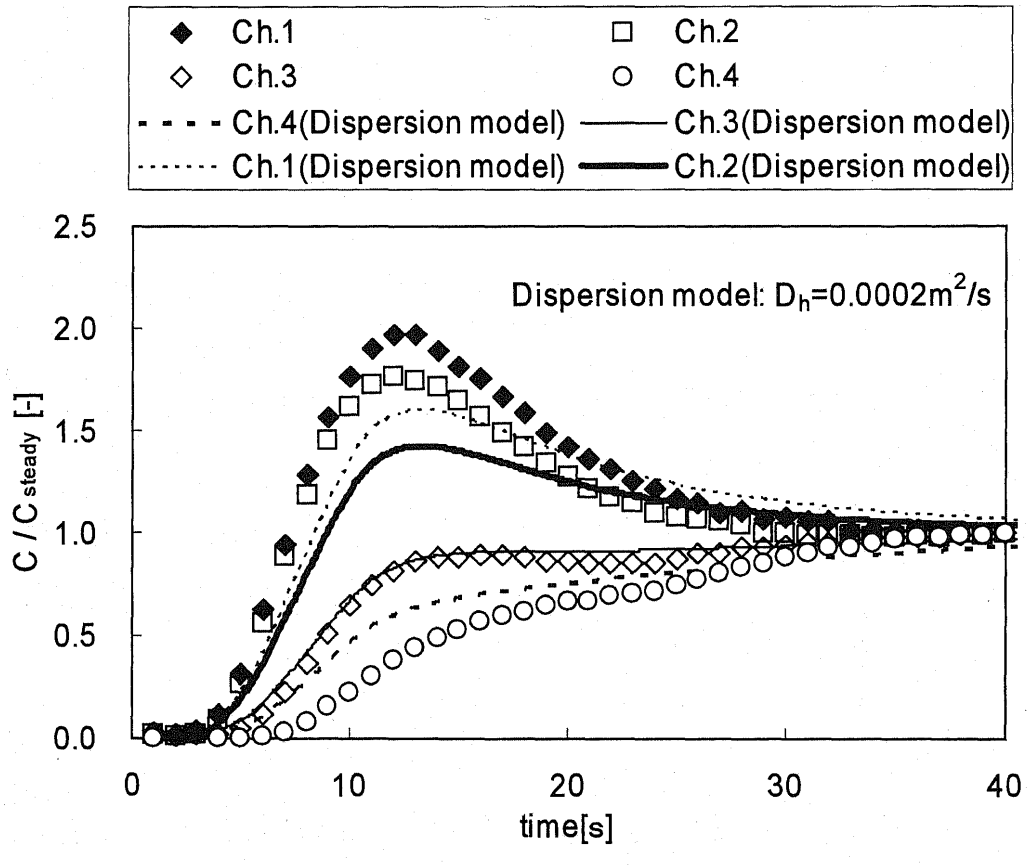

Fig. 3-5 Transient change in CO concentration at different horizontal position after batch injection of activated carbon.

3.5.3 Comparison with literature results

The present experimental results are compared to correlations that have been reported in the literature (Table 3-1). Kunii and Levenspiel [19] derived a horizontal dispersion coefficient by resorting to Einstein's random walk theory (eq. 3-9).

$$D_h = \frac{3}{16}\cdot\frac{\beta}{1-\beta}\cdot\alpha^2 d_b U_{br}\left[\left(\frac{U_{br}+2U_f}{U_{br}-U_f}\right)^{1/3}-1\right]. \tag{3-9}$$

Borodulya et al. [20] developed a sophisticated expression by summarizing experiments using heated tracer particles with a wide range of particle sizes (eq. 3-10):

$$D_h = 0.013(U-U_{mf})H\left(\frac{d_c}{H}\right)^{0.5} Fr^{-0.15}. \tag{3-10}$$

Shi and Fan [21] proposed an empirical correlation of the horizontal dispersion coefficients, which incorporated solid characteristics, operating parameters, and fluidization medium (eq. 3-11):

$$D_h = 0.46(U-U_{mf})H_{mf}\left(\frac{(U-U_{mf})d_p\rho_g}{\mu_g}\right)^{-0.21}\left(\frac{H_{mf}}{d_p}\right)^{0.24}\left(\frac{\rho_p-\rho_g}{\rho_g}\right)^{-0.43} \tag{3-11}$$

Berruti et al [22] measured tracer particle concentrations and developed a modified empirical correlation of the horizontal dispersion coefficient (eq. 3-12):

$$D_h = 0.185\left[1-\left(0.44+2.87\frac{H}{H_{mf}}\right)\left(\frac{l_p}{L/2}\right)^5\right](U-U_{mf})d_p\left(\frac{(U-U_{mf})d_p\rho_g}{\mu_g}\right)^{-0.25}\left(\frac{H_{mf}}{d_p}\right)^{1.45}\left(\frac{\rho_p-\rho_g}{\rho_g}\right)^{-0.43} \tag{3-12}$$

Bellgardt and Werther [12] used of frozen CO_2 solids and estimated the horizontal dispersion coefficient (eq. 3-13):

$$D_h = 0.67 \times 10^{-3} + 0.023 \frac{1}{H} \int_0^H \frac{\beta}{1-\beta} \sqrt{g d_b^3} dh \qquad (3\text{-}13)$$

However, the horizontal dispersion coefficients were found in the order range of 0.0002–0.0003 m^2/s. Two correlations of Kunii & Levenspiel's model assuming bubble size of 0.02 m and Borodulya's model show good agreement for this work while the others give higher value as seen in Table 3-1.

Table 3-1 Comparison of horizontal dispersion coefficient between present measurements and results from the literature

Present result	Shutter method	0.0003	m^2/s
	Batch injection method	0.0002	m^2/s
Kunii and Levenspiel [19]		0.00016	m^2/s
Borodulya et al. [20]		0.00032	m^2/s
Shi and Gu [23]		0.00045	m^2/s
Shi and Fan [21]		0.00059	m^2/s
Bellgardt and Werther [12]		0.00068	m^2/s

3.6 Conclusions

A new tracer technique using carbon-loaded porous bed material tracers has been developed to measure horizontal dispersion of solids mixing in a fluidized bed at high temperature. Two carbon-solid tracers were prepared: using a carbon-loaded bed material with dividing bed using a partition plate, and using activated carbon batch injection. The investigation results within these two experiments show that the horizontal dispersion of solid mixing was evaluated well. The dispersion coefficient was found to be 0.0002–0.0003 m^2/s. Experimental results showed satisfactory agreement with calculations reported in the literature.

Nomenclature

C concentration of CO in gas, %

C_0 concentration of CO in gas before opening shutter (shutter method), %

C_{steady} concentration of CO in gas after complete mixing of tracer, %

D_h horizontal dispersion coefficient, m^2/s

d_b bubble diameter, m

d_c vessel diameter, m

d_p particle diameter, m

F_r Froude number $(U-U_{mf})^2/gH_{mf}$, -

g gravitational acceleration, m/s^2

H bed height, m

H_{mf} minimum fluidization bed height, m

l_p distance from center, m

L horizontal position (from left wall to right in Fig.2), m

t time, s

U superficial gas velocity, m/s

U_{br} bubble rising velocity, m/s

U_f fluidized gas velocity=U_{mf}/ε_{mf}, m/s

U_{mf} minimum fluidizing velocity, m/s

X tracer concentration, mol/m^3

Greek symbols

α parameter in eq.9, value= 0.77

β bubble fraction in dense bed, -

δ Dirac's unit impulse function, -

ε_{mf} vioid fraction under minimum fluidization condition, —

μ_g gas viscosity, kg/(m.s)

ρ_g gas density, kg/m^3

ρ_p particle density, kg/m^3

References

1. R. Bader, J. Findlay, T.M. Knowlton, Gas/solids flow patterns in a 30.5-cm-diameter circulating fluidized bed. In: P. Basu and J.F. Large, Editors, Circulating Fluidized Bed Technology II, Pergamon Press, Oxford 1988.p.123–137.
2. M.J. Rhodes, S. Zhou, T. Hirama, H. Cheng, Effects of operating conditions on longitudinal solids mixing in a circulating fluidized bed riser. AIChE Journal 1991;37: 1450–1458.

3. A. Avidan, J. Yerushalmi, Solids mixing in an expanded top fluid bed, AIChE Journal 1985;31:835–841.

5. F. Wei, W. Chen, Y. Jin, Z.Q. Yu, Lateral and axial mixing of the dispersed particles in CFB. J. Chem. Eng. Jpn. 1995;28;506–510.

4. P.A. Ambler, B.J. Milne, F. Berruti, D.S. Scott, Residence time distribution of solids in a circulating fluidized bed: Experimental and modelling studies. Chem. Eng. Sci. 1990;45:2179–2186.

6. B. Du, F. Wei, Lateral solids mixing behavior of different particles in a riser with FCC particles as fluidized material. Chemical Engineering and Processing 2002;41;329–335.

7. G.S. Grasa, J.C. Abanades, Narrow fluidized bed arranged to exchange heat between a combustion camber and CO_2 sorbent regenerator. Chem. Eng. Sci. 2007;62:619–626.

8. D. Pallares, F. Johnsson, A novel technique for particle tracking in cold 2-dimensional fluidized beds-simulating fuel dispersion. Chem. Eng. Sci. 2006;61: 2710–2720.

9. X. Wei, H. Sheng, W. Tian, Characterizing particle dispersion by image analysis in ICFB. International Journal of Heat and Mass Transfer 2006;49:3338-3342.

10. L.T. Fan, J.C. Song, N. Yutani, Radial particle mixing in gas-solids fluidized beds. Chem. Eng. Sci. 1986;41:117–122.

11. D. Westphalen, L. Glicksman, Lateral solids mixing measurements in circulating fluidized beds. Powder Technology 1995;82:153–167.

12. D. Belgardt, J. Werther, A novel method for the investigation of particle mixing in gas solid systems. Powder Technology 1986;48:173–180.

13. T. Miyauchi, T. Tsutsui, Y. Nozaki, A new fluid thermal cracking process for upgrading residues, presented at AIChE National Meeting, Houston, TX, USA 1987.

14. T. Tsutsui, K. Ijichi, Y. Ikeda, Enhancement of thermal cracking of heavy oil by capacitance effects of porous particles. In: Proc. 8th Symp. on Fluidization. Kitakyushu, Japan: SCEJ;2002.p.452–459.

15. H.J. Franke, T. Shimizu, A. Nishio, H. Nishikawa, M. Inagaki, W. Ibashi, Improvement of carbon burn-up during fluidized bed incineration of plastic pellet using porous bed materials. Energy & Fuels 1999;13:773–777.

16. T. Shimizu, H.J. Franke, S. Hori, T. Yasuo, K. Yamagiwa, M. Tanaka, In-situ hydrocarbon capture and reduction of emissions of dioxins by porous bed material under fluidized bed incineration conditions. In: Pitsupati S, editor. 17th International Conference on FBC, Jack. FL, USA: ASME; 2003.FBC2003-031.

17. T. Shimizu H.J. Franke, H. Satoko, T. Yasuo, K. Yamagiwa, M. Tonsho, M. Inagaki, M. Tanaka, Porous bed material – An approach to reduce both unburnt gas emission and NOx emission from a bubbling fluidized bed waste incinerator. Nihon-Energy Gakkai-Shi 2001;80:331–342.

18. T. Shimizu, H.J. Franke, S. Hori, J. Asazuma, M. Iwamoto, T. Shimoda, S. Ueno, Capacitance effect of porous solids – an approach to improve fluidized bed conversion processes of high-volatile fuels, Chemical Engineering Science 2007;62(18-20):5549-53.

19. D. Kunii, O. Levenspiel, Lateral dispersion of solids in fluidized beds. J. Chem. Eng. Japan 1969;2:122–124.

20. V.A. Borodulya, Y.G. Epanov, Y.S. Teplitskii, Horizontal particle mixing in free fluidized bed, Journal of Engineering Physics 1982;42;528–533.

21. Y. F. Shi, L.T. Fan, Lateral mixing of solids in batch gas-solids fluidized beds. Ind. Chemical Engineering Science 1984;23:337–341.

22. F. Berruti., D.S. Scott, E. Rhodes, Measuring and modeling lateral solids mixing in a three-dimensional batch gas-solid fluidized bed reactor. Can. J. Chemical Engineering 1986;64:48–56.

23. Y. F. Shi, M. X. Gu, Lateral mixing of solids in fluidized beds with partitions, World Congress III of Chemical Engineering, Tokyo, Japan 1986:465–468.

Chapter 4

Model of combustion and dispersion of carbon deposited on porous bed material during bubbling fluidized bed combustion

4.1 Introduction

Fluidized bed combustors (FBCs) using biomass and wastes as fuels for power generation are recognized to have benefits such as the recovery of large amounts of energy remaining in fuels, reducing waste volume, etc. One feature of biomass and wastes as fuels is their high volatile matter content. Because of the high heat transfer from the bed material to fuel, volatile matter evolution occurs very rapidly when fuel is fed into the bed. Consequently, local volatile matter evolution takes place only in the vicinity of the fuel feed point. Complete combustion does not readily occur if the mixing of gas in the upper freeboard is insufficient in fluidized bed combustors. Another problem of local volatile matter evolution is the local heat release in the freeboard, which forms a locally high temperature region and enhances NOx formation. Numerous investigations have been conducted to avoid the problems caused by the high rate of volatile matter evolution. Reducing the bed temperature and reducing gas superficial velocity into the bed engender a lower heating rate during waste combustion [1]. Controlling the waste feed rate

suppresses the fluctuation of volatile matter evolution to maintain desired stoichiometric air ratio [2]; introducing baffles in the freeboard enhances the mixing of air with volatile matter [3].

Another possible measure to suppress the rapid volatile matter evolution is the use of a porous bed material that captures hydrocarbons in the pores as a carbon deposit, by a so-called "capacitance effect" [4 - 12]. It reduces the amount of evolved volatile matter and increases the conversion of carbon in the dense bed. For that reason, it is expected to enhance the horizontal dispersion of carbonaceous materials by solid mixing in the dense bed. It is also expected to inhibit the formation of local fuel-rich zones as well as high-temperature zones in the freeboard [4 - 6]. Another advantage of porous bed material is the lower heat transfer rate from the bed to the fuel. Porous bed material reportedly reduces the heat transfer rate. Consequently, it delays the volatile matter evolution [5, 11, 13, 14].

However, previous investigations have mostly addressed the performance of the porous bed materials for carbon capture; only qualitative experimental results have been obtained using bench-scale combustors. Quantitative analyses incorporating the combustion rate of carbon deposits, the solid dispersion rate, and the horizontal scale of combustor are necessary to apply porous bed materials to

large-scale combustors. In addition, for rational scaling-up of reactors, the removal rate of carbon deposits must necessarily be raised, but information to do so is still lacking. Therefore, it is necessary to establish a model of a bubbling fluidized bed combustor (BFBC) in which both carbon deposit combustion and horizontal solid dispersion occur simultaneously.

In this study, the oxidation rate of carbon deposits is measured by burning carbon deposits with oxygen and measuring the produced CO_2. Based on the burning rate of carbon deposits, a one-dimensional mathematical model of carbon deposit combustion in a bubbling fluidized bed is developed. A two-dimensional mathematical model to predict the horizontal concentration profile of carbon combustion was also developed by taking account of both the reaction rate and solid dispersion. The two-dimensional model was validated through experiments using a two-dimensional fluidized bed combustor by continuously feeding solids with carbon deposits into the reactor.

4.2 Experimental works

This study includes two experiments: 1) measurement of the combustion rate of carbon deposits using a small-scale BFBC; and 2) measurement of the horizontal CO_2 concentration profile in a two-dimensional combustor during continuous

combustion of carbon deposits. The former was conducted in a small BFBC so that carbon deposits can be assumed to disperse uniformly to the horizontal direction. Consequently, only a one-dimensional concentration profile of oxygen along the height of the reactor was examined. The latter was conducted under conditions in which both horizontal solid dispersion and carbon deposit combustion took place.

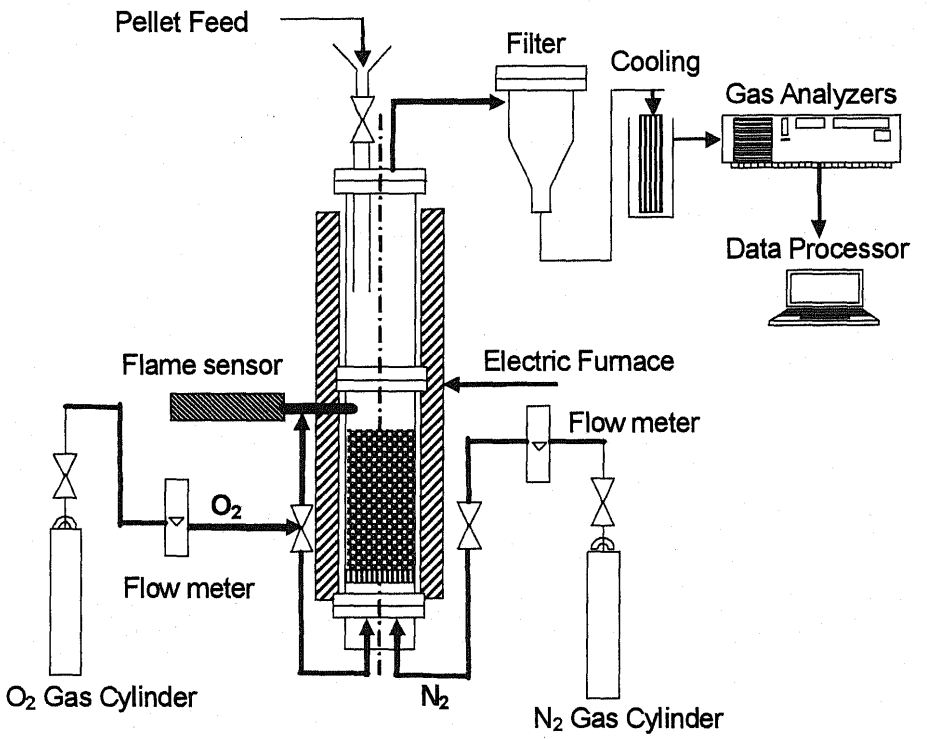

Fig. 4-1 Fluidized bed apparatus to measure burning rate of carbon deposit.

4.2.1 One dimensional BFBC to measure combustion rate of carbon deposit

A schematic diagram of the experimental reactor unit is shown in Fig. 4-1. The bubbling fluidized bed reactor has a 5.3-cm inner diameter. Porous alumina (MS1B, 0.4 mm particle size), whose properties were described elsewhere [4 - 7], was

employed as a bed material with a static bed height of 0.10 m. The bed was fluidized using a nitrogen stream at superficial gas velocities of 0.13 and 0.21 m/s at bed temperatures of 873 K and 943 K. The fuel (polyethylene, PE) pellets were fed from the top of the reactor through a hopper system onto the dense bed. Polyethylene is used as a fuel here because it is known to be converted to 100% volatile matter without forming char [4, 5, 15]. The PE pellets were 4-mm-diameter cylinders. The pellet length was adjusted to obtain the desired weight (approximately 0.15 g for smaller pellets and 0.65 g for larger pellets). Part of the volatile matter released from the fuel pellet was captured by the solids.

The remainder was burned in the freeboard by feeding oxygen at 0.25 m above the distributor, i.e. 0.15 m above the static bed height. After devolatilization, the captured carbon was burned by initiating an oxygen feed from the bottom of the bed through the distributor. The concentration of the combustion product (CO_2) in the flue gas was measured continuously using an NDIR analyzer. The amount of carbon deposited on porous bed material was determined by integrating CO_2 formation. The ratio of the amount of carbon deposit to the carbon in the PE pellet was 0.17 - 0.25 and 0.33 - 0.44 for larger pellets and smaller pellets, respectively. The dynamic response of the gas analyzer was identified by injecting an impulse of CO_2 gas in the gas sampling line. Effect of oxygen concentration on the carbon

burn-up rate was investigated.

4.2.2 Two dimensional BFBC to measure horizontal concentration profile

The laboratory-scale two-dimensional bubbling fluidized bed reactor used for this study is presented in Fig. 4-2. The reactor has a cross section of 0.16 m × 0.04 m and height from the distributor to the top of 0.71 m. The bed material was porous alumina (MS1B, 0.4 mm particle size) with a static bed height of 0.10 m. The bed was operated at temperatures of 873 K and 943 K. During combustion, a mixture of N_2 and O_2 was fed at a superficial gas velocity of 0.13 m/s. The concentrations of O_2 for combustion were 5%, 10%, 15%, and 21%.

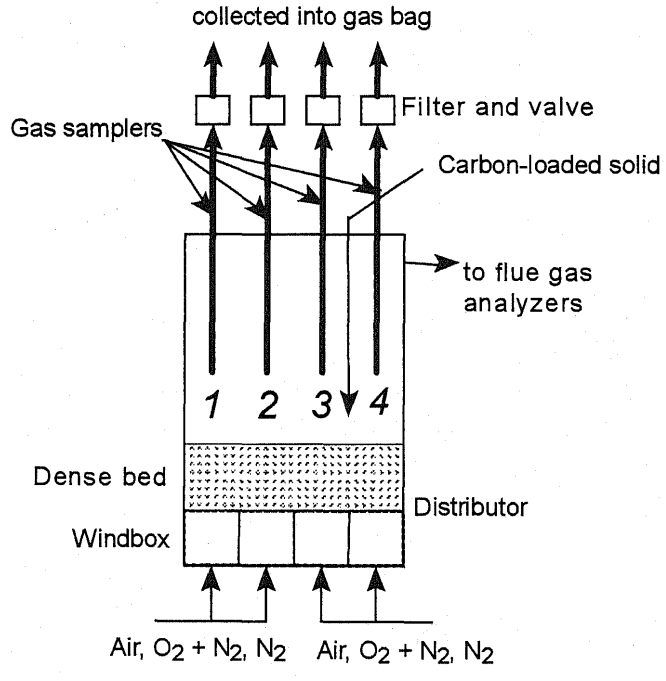

Fig. 4-2 Experimental apparatus for measuring horizontal concentration profile.

Prior to the combustion experiments, carbon-loaded bed material had been prepared using the one-dimensional bubbling fluidized bed reactor described above by feeding PE pellets into solids, when fluidized in a nitrogen stream at 973 K. The carbon-loaded solid was fed continuously from a screw feeder at a distance from the left wall of 0.12 m (L = 0.12) and at a height of 0.15 m above the distributor plate.

Assuming that the CO_2 emission rate from the carbon deposit is proportional to the amount of carbon in the solids, the horizontal concentration profile of carbon in the bed material can be determined by measuring the horizontal CO_2 concentration profile in the freeboard. Four gas-sampling tubes were installed in the freeboard at distances from the left wall of 0.02 m, 0.06 m, 0.10 m, and 0.14 m. The tube inlet height was 0.20 m from distributor plate. The gas samples from the sampling tubes and the flue gas from the reactor top were collected in gas bags and then analyzed using gas chromatography. The horizontal concentration profile of CO_2 released from carbon deposited particles is affected not only by solid dispersion but also by gas mixing. The horizontal gas mixing in the reactor has already been measured in the previous study [16].

4.3. Theory

4.3.1 One-dimensional bubbling fluidized bed reactor

The bubbling fluidized bed model proposed by Kunii and Levenspiel [17] is used to simulate the carbon deposit combustion under conditions of the one-dimensional BFBC experiments. In the one-dimensional BFBC, the horizontal concentration profile of carbon deposit is assumed to be uniform because of its small horizontal cross-sectional area. The vertical concentration profile of carbon deposits is also assumed to be uniform because of vigorous solid mixing induced by rising bubbles. Consequently, only the vertical concentration profile of the gaseous component (oxygen) is examined. The fluidized bed consists of two phases: bubble and emulsion. The exchange of gas between phases is assumed to be of first order with respect to the concentration of gas. For that reason, the change in concentration in the bubble (C_b) and that in the emulsion (C_e) along the bed height is determined as

$$-\delta u_b^{*}(dC_b/dZ) = \delta K_{be}(C_b - C_e) + \delta\gamma_b\rho_c(dX/dt), \qquad (4\text{-}1)$$

and

$$-(1-\delta)u_{mf}(dC_e/dZ) = -\delta K_{be}(C_b - C_e) + (1-\delta)(1-\varepsilon_{mf})\rho_c(dX/dt). \qquad (4\text{-}2)$$

The conversion rate (dX/dt) of the carbon deposit combustion was determined experimentally as a function of carbon conversion X and oxygen concentration C, as explained later. The boundary conditions of eqs. 1 and 2 are given as

$$C_b = C_e = C_{in} \text{ at } Z = 0, \tag{4-3}$$

where C_{in} is the inlet concentration of O_2. Other parameters in eqs.1 and 2 are described below. The gas interchange coefficient between phases (K_{be}) is given as the following relation:

$$K_{be} = 4.5(u_{mf} / d_b) \tag{4-4}$$

where u_{mf} and d_b respectively denote the minimum fluidizing velocity and bubble diameter. A bubble diameter of 2 cm was assumed. The rising velocity of the bubble gas (u_b*) was given by the bubble rise velocity (u_b), the superficial gas velocity (U), and u_{mf}, as the following.

$$u_b^* = u_b + 3u_{mf} \tag{4-5}$$

$$u_b = U - u_{mf} + 0.711(g.d_b)^{0.5} \tag{4-6}$$

In those equations, g denotes gravitational acceleration and δ is the bubble fraction, which is estimated as

$$\delta = (U - u_{mf}) / (u_b + 2u_{mf}). \tag{4-7}$$

The variables ε_{mf} and γ_b respectively represent void fractions in the bed at the minimum fluidizing condition and the volume of solids per unit volume of bubble. They were assumed to be γ_b = 0 and ε_{mf} = 0.45. The carbon concentration (ρ_c) for each cell is calculated in units of kilomoles per cubic meter of solid.

4.3.2 Two-dimensional bubbling fluidized bed reactor

In the two-dimensional bubbling fluidized bed, vertical mixing of solids is assumed to be very good because of the vertical motion of bubbles, although horizontal solid dispersion is poor. Thereby, the solid dispersion can be treated as a one dimensional diffusion model to the horizontal direction. For modeling, the reactor is divided horizontally into J cells so that the horizontal cross sectional area can be sufficiently small and the horizontal concentration of carbon deposit in each cell can be treated as uniform. Also, the particles are assumed to be completely mixed in the vertical direction. The mass flow rate of carbon deposit by solid dispersion in each cell is calculable as follows:

$$N_i = D_h A(1-\delta)(1-\varepsilon_{mf})\left(\frac{\rho_{c,i+1}-\rho_{c,i}}{\Delta L} - \frac{\rho_{i,1}-\rho_{c,i-1}}{\Delta L}\right) \quad \text{for } i = 2,\ldots, J\text{-}1 \quad (4\text{-}8)$$

where D_h is the horizontal dispersion coefficient, A is area of the interface between neighbouring cells, ΔL is the horizontal length in each section and $\rho_{c,i}$ is the carbon concentration. At both ends of the reactor (i = 1 and J), the carbon mass flow through the wall is zero; consequently, the mass flow of carbon deposit is

$$N_1 = D_h A(1-\delta)(1-\varepsilon_{mf})\left(\frac{\rho_{c,2}-\rho_{c,1}}{\Delta L}\right) \quad (4\text{-}9)$$

$$N_J = D_h A(1-\delta)(1-\varepsilon_{mf})\left(\frac{\rho_{c,J-1}-\rho_{c,J}}{\Delta L}\right). \quad (4\text{-}10)$$

A previous work [16] reported the solid dispersion coefficient as D_h = 0.0002 - 0.0003 m^2/s under the same conditions as those of the present work. Smaller value

of D_h = 0.0002 m^2/s was obtained by batch injection of tracer particles at L = 0.12 m, whereas larger value of D_h =0.0003 m^2/s was obtained by shutter method.

The two-dimensional BFBC experiments were carried out under continuous carbon-loaded solid feed conditions. Therefore, the carbon feed rate was added to the mass flow of carbon at the cell below the solid feed point in the present model. From the rate of mass flow of carbon deposit by dispersion and the rate of carbon consumption by combustion, the change in carbon concentration was calculated for each cell over time. Calculations were repeated until a steady state was attained. The bed was divided into 8 cells (ΔL = 2cm) or 16 cells (ΔL =1cm) along horizontal position, but no significant differences in horizontal CO_2 concentration profile were observed between these two configurations. The horizontal concentration profile of CO_2 released from carbon deposited particles is affected not only by solid dispersion but also by horizontal gas mixing in the freeboard, as reported previously [16]. The gas dispersion is also taken into consideration in the same manner as the previous work.

4.4. Results and Discussion

4.4.1 Measurement of the combustion rate using a one-dimensional BFBC model

The rate expression of carbon deposit combustion must be determined for the fluidized bed model. When carbon-loaded solids are exposed to O_2 at high temperatures, the carbon forms CO_2 as

$$C + O_2 \rightarrow CO_2. \qquad (4\text{-}11)$$

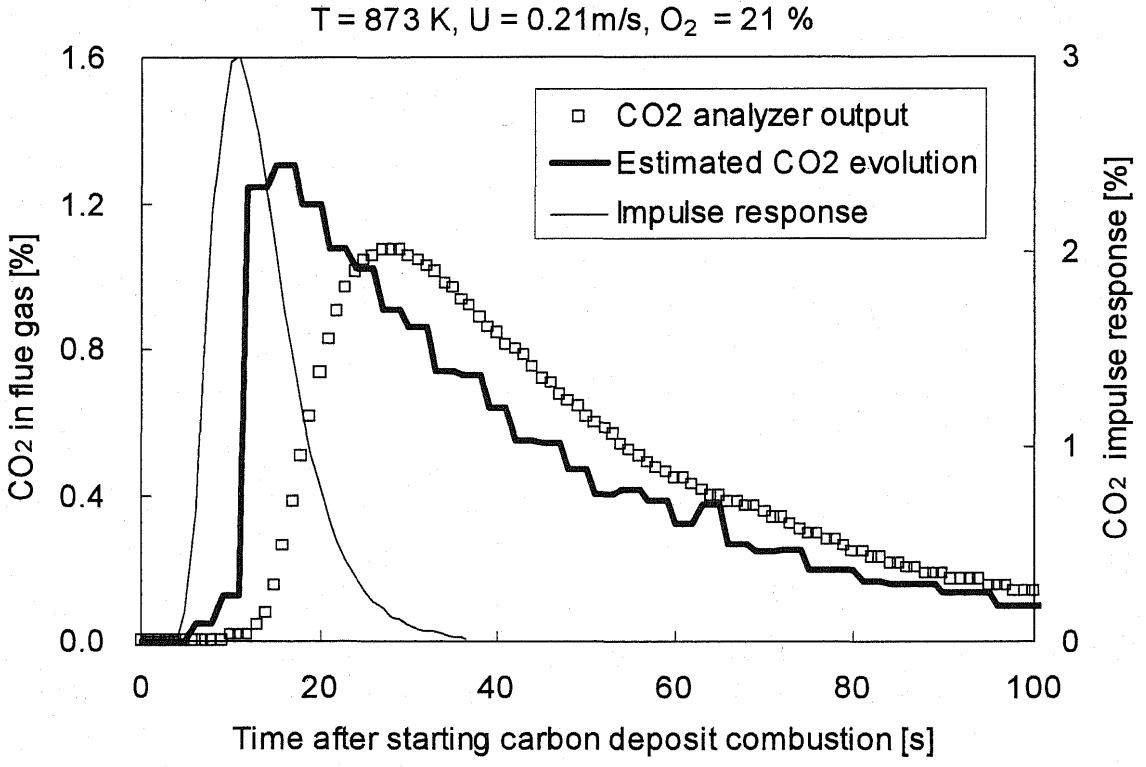

Fig. 4-3 Transient change in CO_2 evolution rate during carbon deposit combustion in one-dimensional BFBC.

Fig. 4-3 shows a typical result of CO_2 evolution during carbon deposit combustion. At first, the dynamic response of CO_2 analyzer was identified by injecting CO_2 impulse in the gas sampling line. The relationship between the true CO_2

concentration in the flue gas and the output signal of the analyzer is given by the convolution with the impulse response as follows:

$$Y_{out}(t) = \int_{-\infty}^{t} Y_{true}(\tau) f(t-\tau) d\tau \,. \qquad (4\text{-}12)$$

The true CO_2 evolution rate during deposit combustion was then estimated by correcting the output signal of the analyzer by solving eq.4-12. Because the estimation of true CO_2 evolution rate is equivalent to high-frequency compensation, high-frequency noise in the output signal is also amplified. To suppress the amplification of the noise, temporal resolution was reduced from 1 s for the measured output signal to 3 s for the estimated true CO_2 concentration. The estimated CO_2 evolution is shown in Fig. 4-3. After an introduction period, which is attributable to the gas residence time in the reactor, steep increase in the estimated CO_2 concentration was observed. Then the concentration gradually decreased with time, i.e., the combustion rate decreased with carbon burn-up. The rate of the increase in the estimated CO_2 concentration just after the introduction period was sufficiently higher than the rate of the decay of CO_2 concentration during combustion. Therefore, the influence of back mixing of gas in the reactor on the evaluation of carbon combustion rate is considered to be negligible.

Based on the estimated true CO_2 evolution rate, carbon combustion rate was determined. As shown in Fig. 4-4, $ln(1 - X)$ had a straight-line relationship with

time after the initial introduction period. Thus the conversion rate (dX/dt) was found to be proportional to the unreacted fraction (1 - X) as:

$$dX/dt = k(1-X). \qquad (4\text{-}13)$$

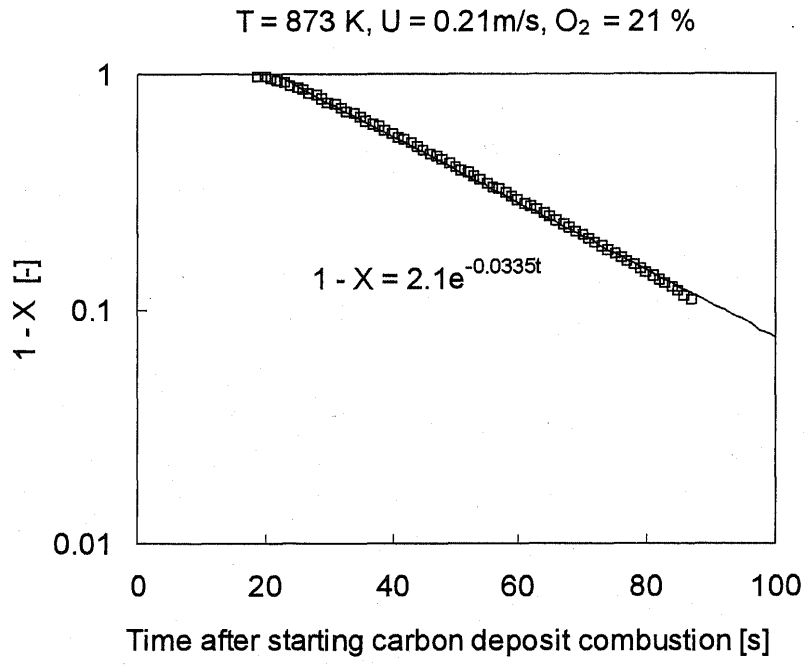

Fig. 4-4 Change in carbon conversion (X) during carbon deposit combustion (one-dimensional BFBC).

Figure 4-5 shows the effects of temperature, oxygen concentration, superficial gas velocity, and mass of fuel pellet on the parameter k. The parameter k was determined as

$$k = k_0 C^n, \qquad (4\text{-}14)$$

where C is the O_2 concentration. The apparent reaction order n at 843 K was 0.55, which suggests that the combustion took place under a condition of chemical kinetic control; if the mass transfer resistance was the rate-controlling step, the apparent

reaction order would be unity because the mass transfer rate is proportional to the concentration of oxygen. At 943 K, the apparent reaction order obtained under a condition of a superficial gas velocity of 0.21 m/s and feeding of smaller fuel pellets (ca. 0.15 g) was 0.63. However, at 943 K under a lower gas velocity (0.13 m/s) condition or under a larger fuel pellet (0.65 g) feeding condition, the apparent reaction rate became smaller. The reduced reaction rate is considered to result from the reduced oxygen concentration in the emulsion phase resulting from the consumption of oxygen by carbon combustion. Therefore, numerical analysis is necessary to evaluate the validity of the reaction rate given in Fig. 4-5 as:

$$k = 0.75C^{0.55} \quad \text{(at 873 K)} \tag{4-15}$$

$$k = 4.32C^{0.63} \quad \text{(at 943 K).} \tag{4-16}$$

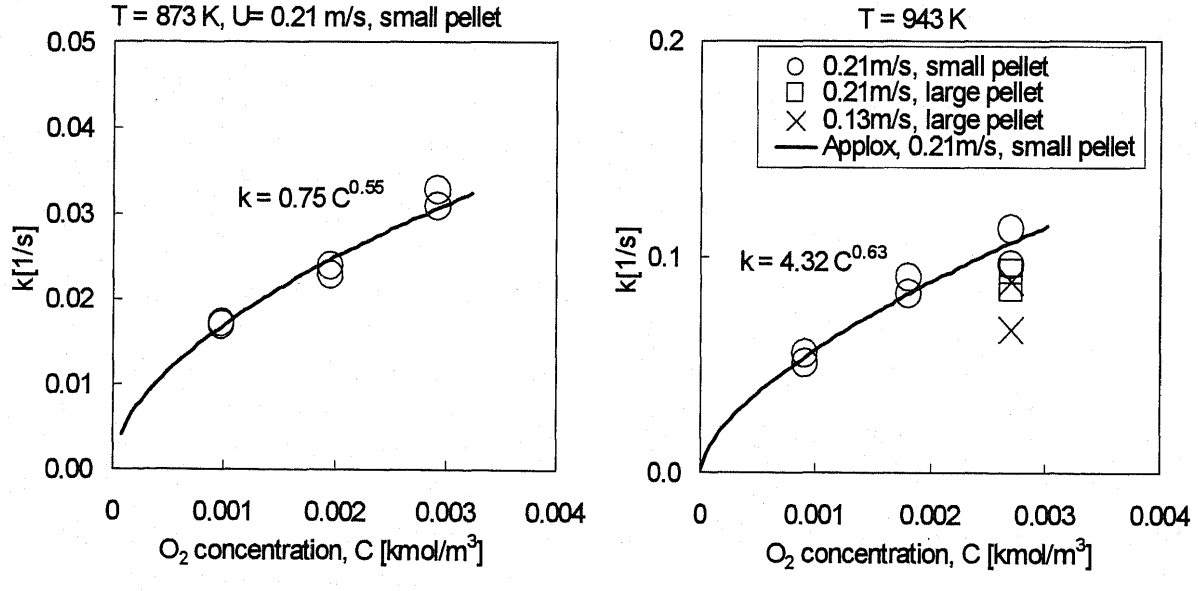

Fig. 4-5 Effect of operating conditions and oxygen concentration on *k*.

The reaction rate expressions of the reaction kinetic for combustion of carbon deposit (eqs. 4-15 and 4-16) were integrated in the one-dimensional fluidized bed model; then the concentration profile of O_2 along the bed height was calculated. Figure 6 shows the change in the O_2 concentration along the bed height. The change in the O_2 concentration along the bed height was considerably high and the concentration difference between C_b and C_e was also notably high when burning PE pellets of 0.65 g at a superficial gas velocity of 0.13 m/s. Calculations were also made for the case of burning smaller PE pellets of 0.15 g at a higher velocity of 0.21 m/s. The change in the O_2 concentration along the bed height was found to be small, in addition to the concentration difference between C_b and C_e.

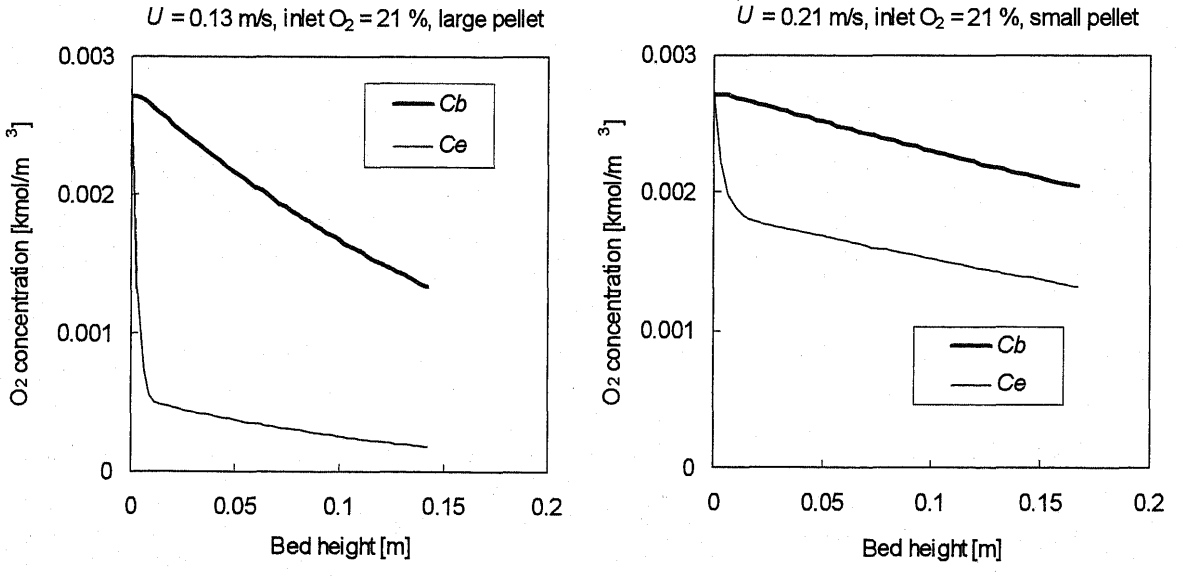

Fig. 4-6 Calculated concentration profile along bed height by one-dimensional model (temperature = 943 K, t = 0).

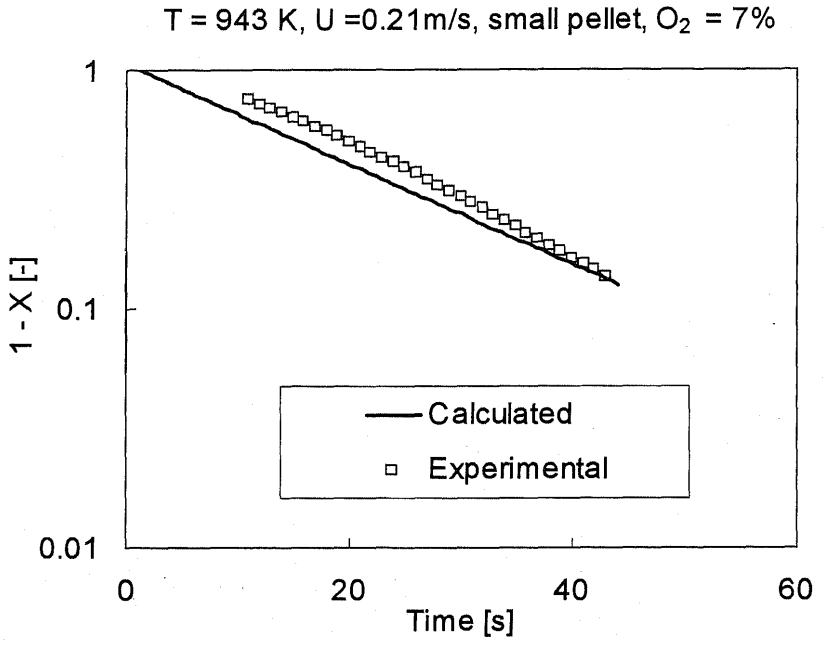

Fig. 4-7 Comparison of the change in unreacted fraction of carbon with time between model and experiment.

The transient change in CO_2 concentration in the flue gas was also calculated using the present one-dimensional model. The calculated change in unreacted fraction of carbon was also approximated by rate expression eq.4-12 (Fig. 4-7). The calculated apparent reaction rate constant, *k*, agreed with the experimental results as shown in Fig. 4-8, regardless of the experimental conditions. Therefore, the rate expression that had been obtained from the condition by burning PE pellet at amount of 0.15 g at a superficial gas velocity of 0.21 m/s was adopted for the two-dimensional model.

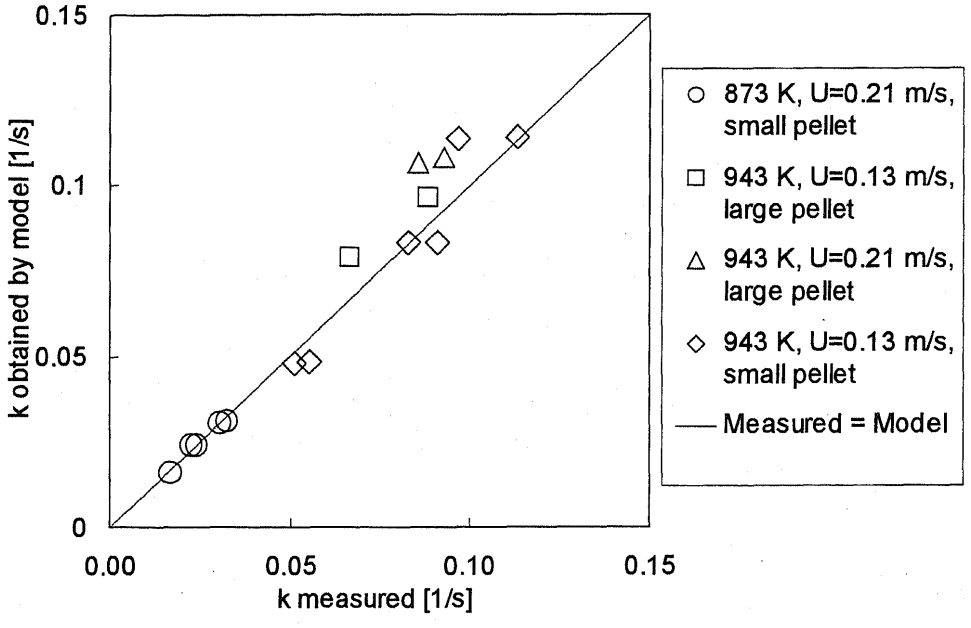

Fig. 4-8 Comparison between experimentally obtained apparent reaction rate constant *k* and that calculated by one-dimensional fluidized bed model.

4.4.2 Horizontal concentration profile of CO_2 in two-dimensional bubbling fluidized bed

Figure 4-9 shows a comparison between experimental results and a two-dimensional model of the horizontal concentration profile of CO_2 in the freeboard.

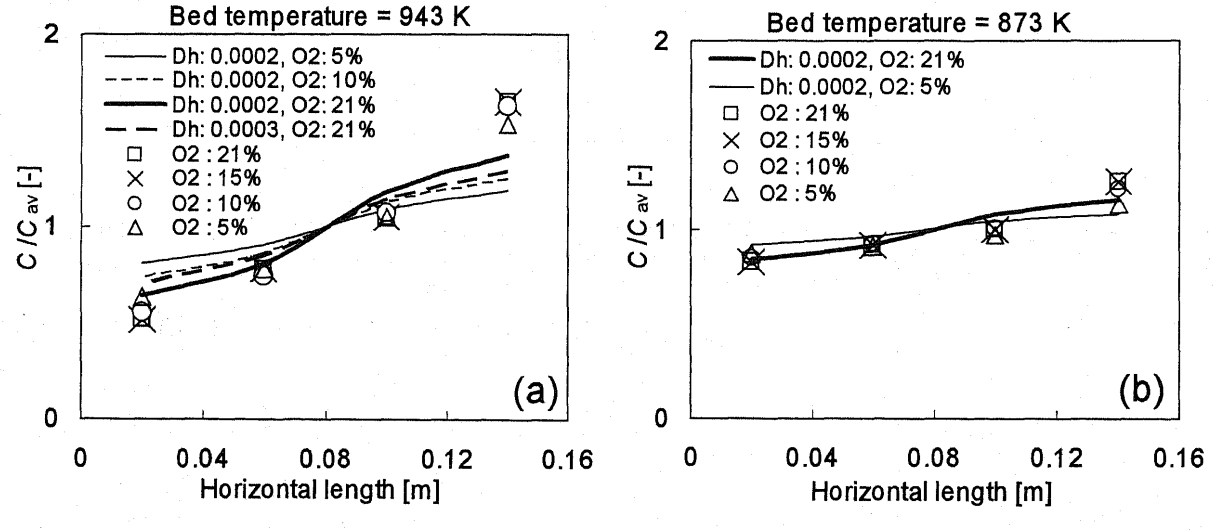

Fig. 4-9 Horizontal profile of CO_2 concentration at upper surface of bed (Comparison of experiment results and two-dimensional model).

In this figure, the concentration was normalized by the average concentration, C_{av}. The model results agreed satisfactorily with experimental results. The horizontal concentration profile of carbon is determined by the relative importance of solid dispersion and carbon consumption by combustion. For the lower temperature of 873 K, the dispersion of carbonaceous material became uniform as a result of the low combustion rate. With increasing temperature, the combustion rate increases, and the carbon is consumed in the vicinity of the fuel feed point. For that reason, a non-uniform horizontal concentration profile was observed at 943 K. In contrast to the effect of temperature, the influence of oxygen concentration on the horizontal concentration profile was minor, which is attributable to the low reaction order with respect to oxygen concentration. At 943 K, the calculation result for a dispersion coefficient of D_h = 0.0002 m^2/s gave better agreement with the experimental results than that for D_h =0.0003 m^2/s. The smaller value of D_h = 0.0002 m^2/s was obtained by batch injection of tracer particles at L = 0.12 m [16], which is the same feeding position of carbon-loaded particles as the present experiments. A larger value of D_h =0.0003 m^2/s was obtained by shutter method, in which the movement of shutter might enhance solid mixing.

Both the reaction rate of carbon deposit combustion and the solid dispersion are clearly important in order to predict the carbon dispersion behaviour in a large-scale

combustor. As the first step to scaling-up of the FBC system using carbon loaded solids prepared by capacitance effect, these two factors are examined simultaneously in the present work in a fundamental manner. The present model is considered to be applicable to large-scale BFBCs if the solid dispersion coefficient can be predicted.

The carbon concentration profile without taking account of gas mixing is also provided as seen in Fig. 4-10. Here, the solid dispersion coefficient as D_h = 0.0003 m^2/s gave a good agreement with the model calculations.

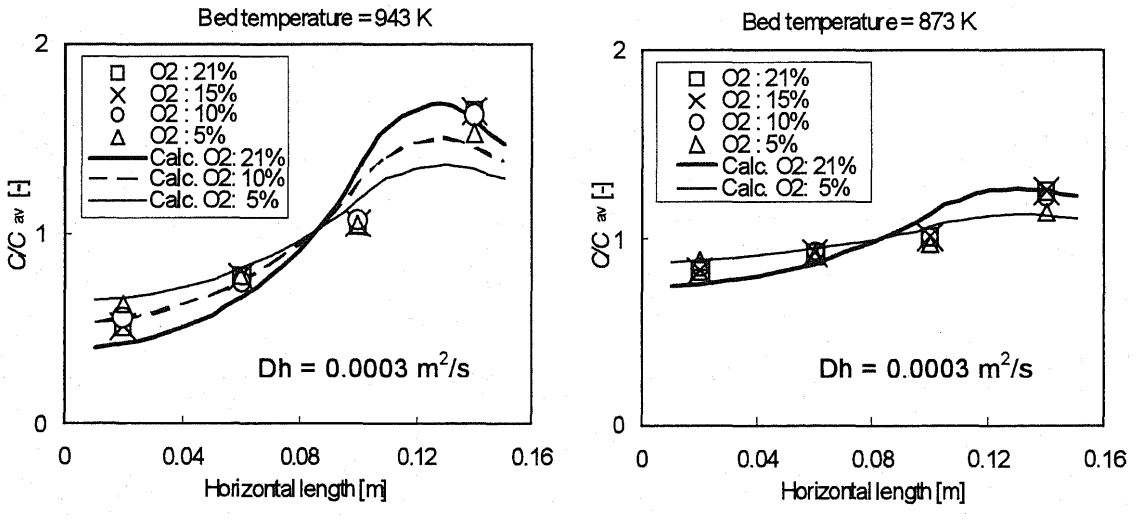

Fig. 4-10. Comparison of experimental results and those of the two-dimensional model.

The comparison is also made to correlation of dispersion coefficient models reported in the literatures such as Kunii and Levenspiel [17], and Bellgardt and Werther [18] as shown in Figure 4. The dispersion coefficients were 0.00016 m^2/s

and 0.00068 m^2/s respectively. It is found more uniform horizontal concentration profile at higher dispersion coefficients and for lower oxygen concentration.

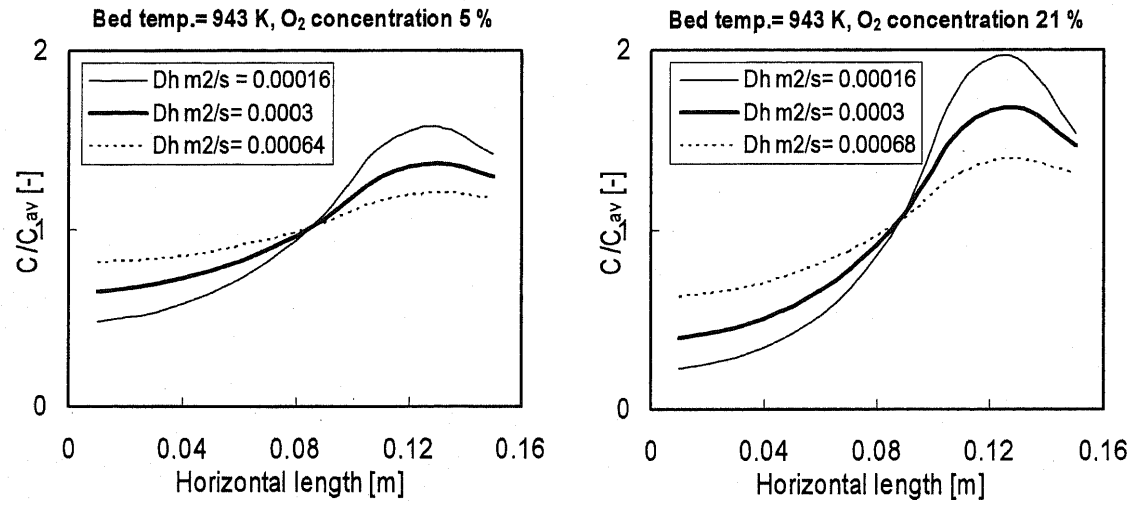

Fig. 4-11. Comparison of the present two-dimensional model and the published dispersion coefficient models.

4.5. Conclusions

Mathematical models were developed for combustion of carbon deposits after preparation by contacting volatile matter with the porous alumina bed material under FBC conditions in laboratory-scale one-dimensional and two-dimensional fluidized bed reactors. The reaction rate of carbon deposit combustion was measured using a BFBC with 5.3 cm inner diameter. The reaction rate and carbon dispersion were included through an overall material balance. Then a mathematical model was developed to predict the horizontal concentration profile. Validation was made by conducting experiments using a two-dimensional bubbling fluidized bed to

evaluate the horizontal concentration profile of CO_2 produced in the freeboard. Agreement was observed between results obtained using the two-dimensional model and experiments. For an initial study of combustion of carbon-loaded solids prepared by the capacitance effect, this information is important for scaling-up purposes of commercial bubbling fluidized beds.

Nomenclature

A interface area between neighbouring cells, m^2

C O_2 concentration, $kmol/m^3$

C_b O_2 concentration in the bubble phase, $kmol/m^3$

C_e O_2 concentration in the emulsion phase, $kmol/m^3$

C_{av} average concentration, $kmol/m^3$

C_{in} O_2 concentration in the inlet, $kmol/m^3$

D_h horizontal dispersion coefficient, m^2/s

d_b bubble diameter, m

$f(t)$ impulse response of CO_2 analyzer, 1/s

g gravitational acceleration, m/s^2

J number of cells, -

K_{be} gas interchange coefficient between bubble and emulsion, 1/s

k the apparent reaction rate constant with respect to the unreacted fraction of solids eq. 13, 1/s

k_0 reaction rate constant in eq. 14, $1/ ((kmol/m^3)^n s)$

L horizontal position in two-dimensional fluidized bed, m

N mass flow rate of carbon by dispersion, kmol/s

n reaction order with respect to oxygen concentration in eq. 14

T bed temperature, K

t time, s

U superficial gas velocity, m/s

u_b bubble rise velocity, m/s

u_b^* rising velocity of the bubble gas, m/s

u_{mf} minimum fluidizing velocity, m/s

X the fractional conversion of carbon, -

$Y_{true}(t)$ true CO_2 concentration in the flue gas

$Y_{out}(t)$ output signal of CO_2 analyzer

Z height, m

Greek symbols

γ_b volume of solids per unit volume of bubble, -

δ bubble fraction in dense bed, -

ε_{mf} void fraction under minimum fluidization condition, -

ρ_c carbon concentration in solids, kmol/m^3-solid

References

1. N. Fujiwara, M. Yamamoto, T. Oku, K. Fujiwara, S. Ishii, CO reduction by mild fluidization for municipal waste incinerator. In: Proc. of 1st SCEJ Symposium on Fluidization. Tokyo, Japan: SCEJ; 1995.p.51-5.

2. K. Koyama, M. Suyari, F. Suzuki, M. Nakajima, Combustion technology of municipal fluidized bed technology. In: Proc. of 1st SCEJ Symposium on

Fluidization. Tokyo, Japan: SCEJ; 1995.p.56-63.

3. T. Izumiya, K. Baba, J. Uetani, H. Hiura, M. Furuta, Experimental study of combustion and gas flow at freeboard of fluidized combustion chamber for municipal waste. In: Proc. of 3rd SCEJ Symposium on Fluidization. Nagoya, Japan: SCEJ; 1997.p.210-5.

4. H.J. Franke, T. Shimizu, A. Nishio, H. Nishikawa, M. Inagaki, W. Ibashi, Improvement of carbon burn-up during fluidized bed incineration of plastic by using porous bed materials. Energy & Fuels 1999;13:773-7.

5. H.J. Franke, T. Shimizu, S.Hori, Y. Takano, M. Tonsho, M. Inagaki, M.Tanaka, Simultaneous reduction of NOx emission and unburnt hydrocarbon emission during plastic incineration in fluidized bed combustor. In: Donald W, Geiling PE, editor. 16th International Conference on FBC. New York, USA: ASME; 2001.FBC2001-94.

6. T. Shimizu, H.J. Franke, S. Hori, Y. Takano, M. Tonsho, M. Inagaki, M. Tanaka, Porous bed material – An approach to reduce both unburnt gas emission and NOx emission from a bubbling fluidized bed waste incinerator. Journal Japan Inst. Energy 2001;80:333-42.

7. T. Shimizu, H.J. Franke, S. Hori, T. Yasuo, K. Yamagiwa, M. Tanaka, In-situ hydrocarbon capture and reduction of emissions of dioxins by porous bed

material under fluidized bed incineration conditions. In: Pitsupati S, editor. 17th International Conference on FBC, Jacksonville FL, USA: ASME; 2003.FBC2003-031.

8. T. Namioka, K. Yoshikawa, H. Hatano, Y. Suzuki, High tar reduction with porous particles for low temperature biomass gasification: Effects of porous particles on tar and gas yields during sawdust pyrolysis. J. Chem. Eng. Japan 2003;36:1440-8.

9. K. Ito, Moritomi H, Yoshiie R, Uemiya S, Nishimura M. Tar capture effect of porous particles for biomass fuel under pyrolysis conditions. J. Chem. Eng. Japan 2003;36:840-5.

10. T. Teramae, Effect of catalysis on tar elimination and gas production from fluidized bed gasification of biomass. Kagaku Kogaku Ronbunshu 2007;33:257-60.

11. I N.S. Winaya, T. Shimizu, Reduction of volatile matter evolution rate from a plastic pellet during bubbling fluidized bed pyrolysis by using porous bed material. Chemical Engineering and Technology 2007;30(8):1003-9 DOI:10.1002/ceat.200600309.

12. T. Shimizu, H.J. Franke, S. Hori, J. Asazuma, M. Iwamoto, T. Shimoda, S. Ueno, Capacitance effect of porous solids – an approach to improve fluidized bed

conversion processes of high-volatile fuels. Chemical Engineering Science 2007;62(18-20):5549-53, DOI:10.1016/j.ces.2006.12.015.

13. H.J. Franke, T. Shimizu, S. Hori S, Y. Takano, M. Tonsho, M. Inagaki, M. Tanaka, Suppression of rapid devolatilization of plastic during bubbling fluidized bed combustion using porous bed material. In: 3rd European Conference on Fluidization. Toulouse, France; 2000.p.641-8.

14. Reduction of devolatilization rate of fuel during bubbling fluidized bed combustion using porous bed material. Chemical Engineering and Technology 2001;24(7):725-33.

15. J. Baron, E.M. Bulewicz, S. Kandefer, M. Pilawska, W. Żukowski, A.N. Hayhurst, The combustion of polymer pellets in a bubbling fluidised bed. Fuel 2006;85(17-18):2494-508.

16. I N.S. Winaya, T. Shimizu, D. Yamada, A new method to evaluate horizontal solid dispersion in a bubbling fluidized bed. Powder Technology 2007; 178(3):176-81 DOI:10.1016/j.powtec.2007.05.005.

17. D. Kunii, O. Levenspiel, Fluidization Engineering (2nd Edition). Stoneham: Butterworth-Heinemann; 1991.p.277.

18. D. Belgardt, J. Werther, A novel method for the investigation of particle mixing in gas solid systems, Powder Technology 48 (1986) 173–180.

Conclusion

Some counter measures have been applied by many researchers to suppress emission of unburnt gases caused by rapid VM evolution from using biomass and wastes fuel in fluidized bed combustion.

In Chapter 1, the characteristic of biomass and wastes fuels and their counter measures has been summarized. The purposes of the present studies were also discussed.

In Chapter 2, the effect of bed material on the onset of devolatilization was measured by use of a bench-scale bubbling fluidized bed reactor. Various porous bed materials were employed in fluidized bed combustor of pellet fuel to evaluate the effect of volatile matter capture and heat transfer coefficient to the delay of devolatilization. The onset of devolatilization was found to delay by employing porous bed materials compared to non-porous quartz sand. Volatile matter capture (capacitance effect) and heat transfer coefficient of the porous solids bed were also measured. The onset of devolatilization was mainly determined by the heat transfer rate, whereas the capacitance effect had no influence on the delay of the devolatilization.

In Chapter 3, a new tracer technique using carbon-loaded porous bed material

tracers has been developed to measure horizontal dispersion of solids mixing in fluidized bed at high temperature that resemble those of commercial operations. Two ways of carbon-solid tracers were employed; by employing carbon-loaded bed material with dividing bed using partition plate and by using activated carbon batch injection. The investigation results within these two experiments show that the horizontal dispersion of solid mixing was evaluated well. The experimental results were in satisfactory agreement with the literature calculations.

In Chapter 4, the intrinsic proposed model which includes the reaction rate of carbon deposit combustion and the solid dispersion has been validated. As the first step to scaling-up of the FBC system using carbon loaded solids prepared by capacitance effect, these two factors are examined simultaneously in the present work in a fundamental manner. The present model is considered to be applicable to large-scale BFBCs if the solid dispersion coefficient can be predicted.

In Chapter 5, this work is summarized. The work is considered to cover some essential innovations on FBC of high-volatile fuels. The result of this thesis is possible to apply for scale-up purposes of commercial bubbling fluidized bed using porous solids as a bed material.

APPENDIX A1

Calculation for horizontal gas mixing

The horizontal gas mixing was evaluated by using pure CO_2 as a tracer gas. The CO_2 gas with concentration of 5% in average was injected at different vertical positions of 0.00 m, 0.05 m and 0.10 m above the distributor plate and different horizontal positions of 0.01 m, 0.04 m and 0.08 m from the left wall. The sample gas from each probe was collected in a gas bag then analyzed using a gas chromatography.

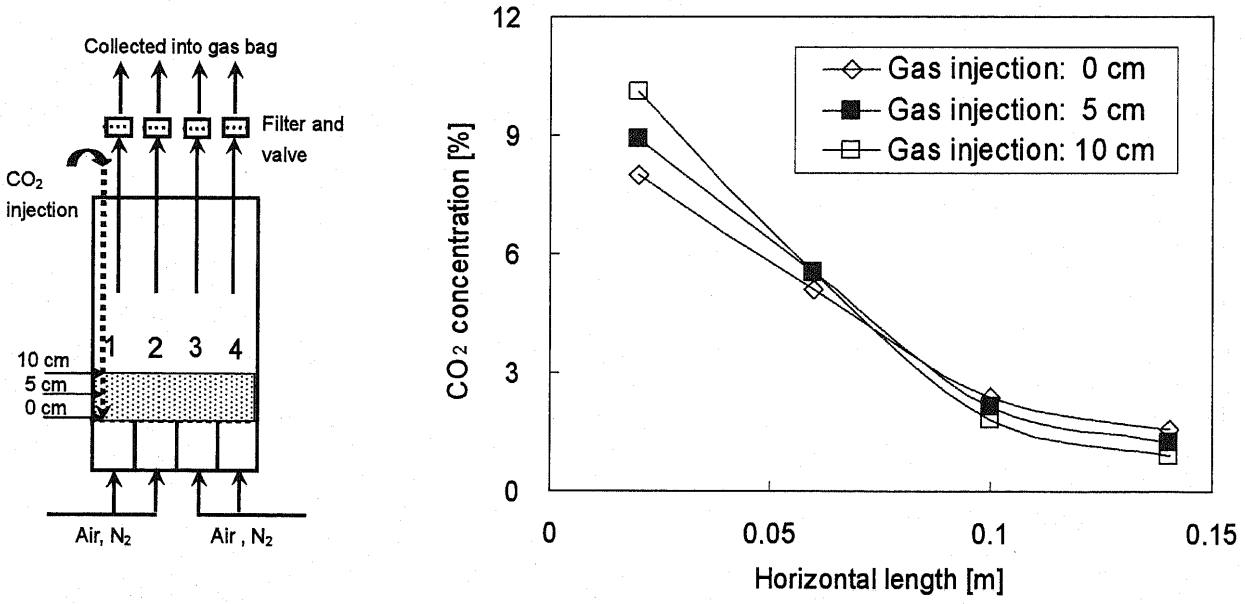

Fig A.1 Gas mixing from horizontal position of 0.01 m at different vertical injection points above distributor plate.

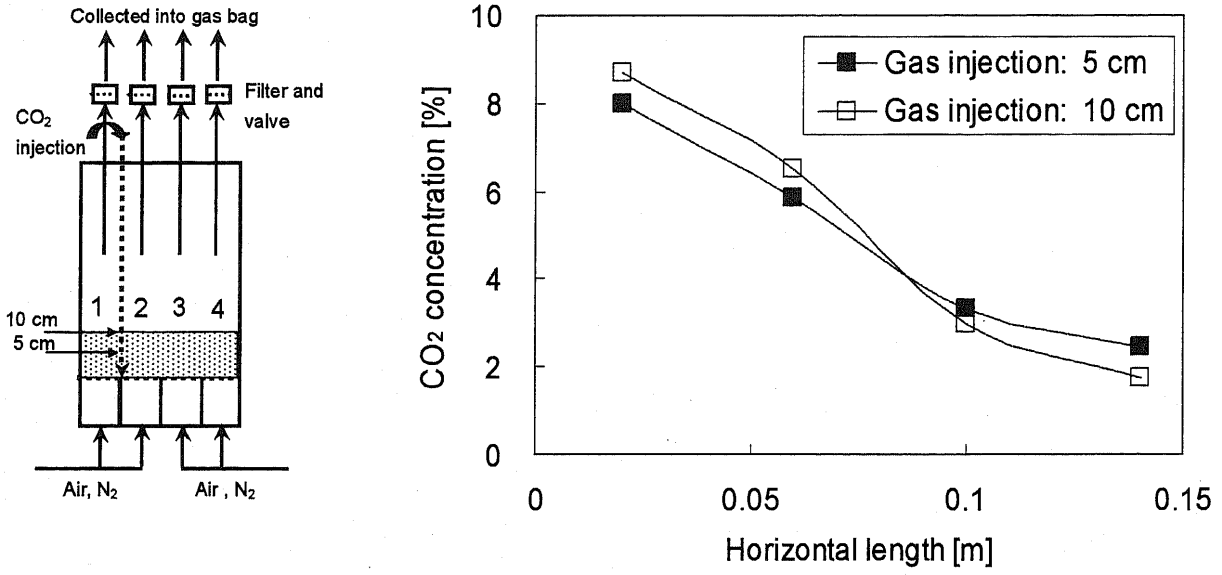

Fig A.2 Gas mixing from horizontal position of 0.04 m at different vertical injection points above distributor plate.

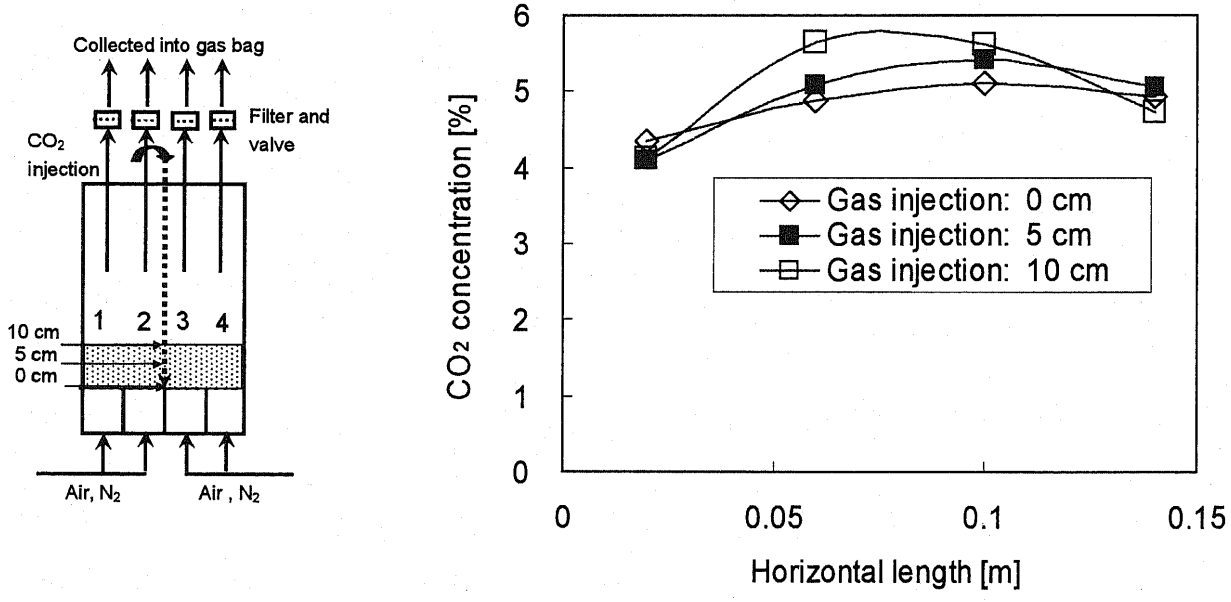

Fig A.3 Gas mixing from horizontal position of 0.08 m at different vertical injection points above distributor plate.

The experimental results as shown in Fig. A1, Fig. A2 and Fig A.3 were then summarized in Fig. A4. The CO_2 gas concentration was normalized by the average concentration.

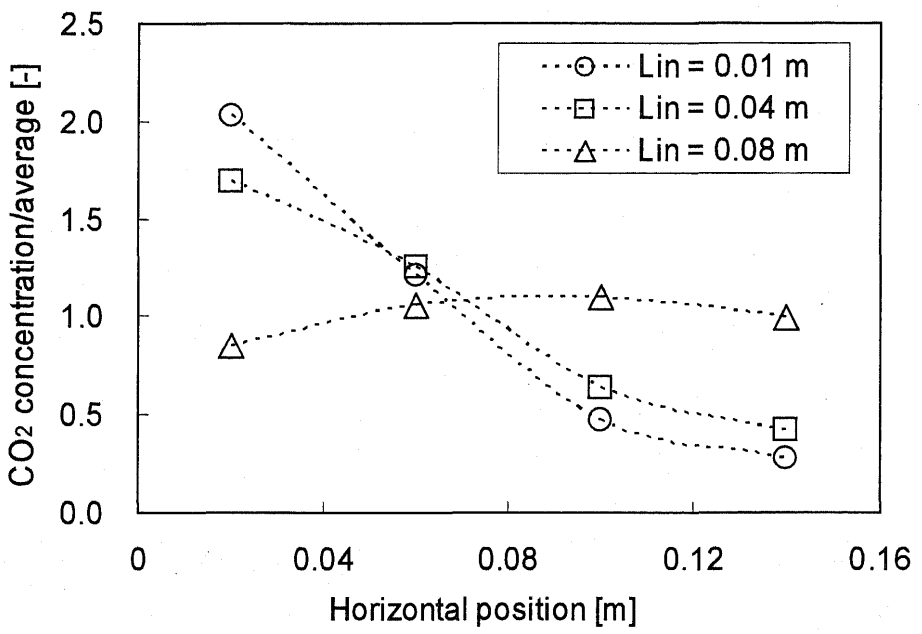

Fig A.4 Gas mixing along horizontal position at different injection points (Lin)

Table A.1 The summarized results of gas mixing experiments

Injection point	Probe position [m]			
Lin, m	**0.02**	**0.06**	**0.1**	**0.14**
0.01	2.03	1.21	0.48	0.28
0.04	1.69	1.25	0.64	0.42
0.08	0.85	1.06	1.10	1.00

To include the effect of the theoretical concentration profile of the gas mixing into the model of calculations, the numerical equations are drawn from table A.1. The equations are shown in the Fig. A and they are rewritten as eq. A1 to A4.

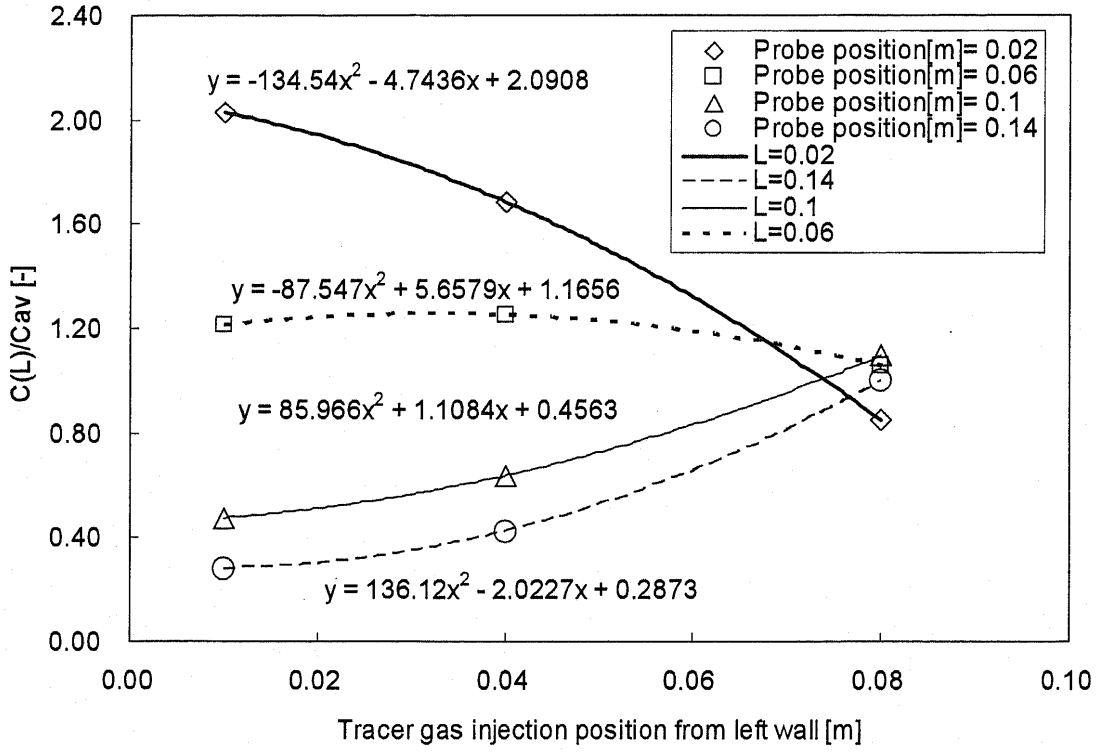

Fig A.5 Gas mixing along horizontal position at different injection points

The equations for each horizontal position (channel) of 0.02 m, 0.06 m, 0.10 m and 0.14 m are:

$$Ch.1 = X(0.02) = -134.54x^2 - 4.7436x + 2.0908 \quad (A.1)$$

$$Ch.2 = X(0.06) = -87.547x^2 + 5.6579x + 1.1656 \quad (A.2)$$

$$Ch.3 = X(0.10) = 85.966x^2 + 1.1084x + 0.4563 \quad (A.3)$$

$$Ch.4 = X(0.14) = 136.12x^2 - 2.0227x + 0.2873 \quad (A.4)$$

By dividing the bed into 32 of 0.005 m in each cell, the horizontal gas concentration profile along the bed in each channel is obtained as below:;

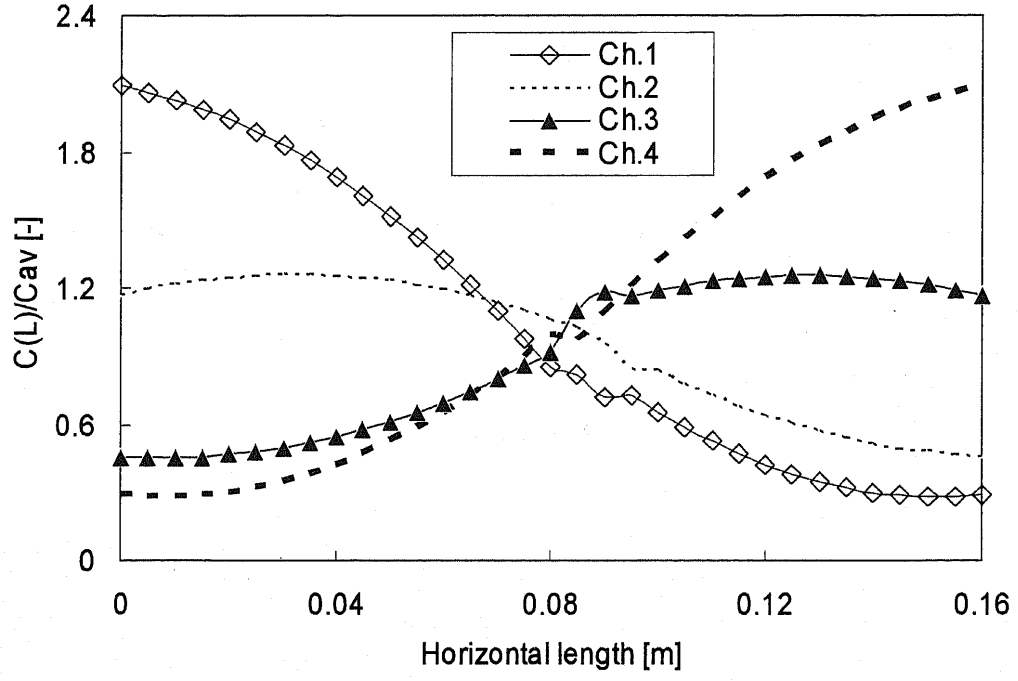

Fig A. 5 Gas concentration profile along horizontal position in each channel.

The time step of calculation (Δt) is obtained from:

$$\frac{D_h \Delta t}{(\Delta L)^2} = \frac{1}{2} \qquad \text{(A-5)}$$

where ΔL denotes distance between neighboring locations = 0.005 m. While D_h is horizontal coefficient dispersion, so the transient change in X with a time step of Δt is given as eq. 3-5.

$$X(t+\Delta t, L) = \frac{X(t, L+\Delta L) + X(t, L-\Delta L)}{2} \qquad \text{(A-6)}$$

By solving eq. A-6, the change in X with time is calculated numerically.

APPENDIX A2

Horizontal dispersion without gas mixing effect.

Without taking account of a gas mixing effect, the transient change concentration profile of CO is presented as below. For shutter method of probe #1, by giving a value of D_h = 0.0005 m^2/s, the experimental results agreed with the diffusion model.

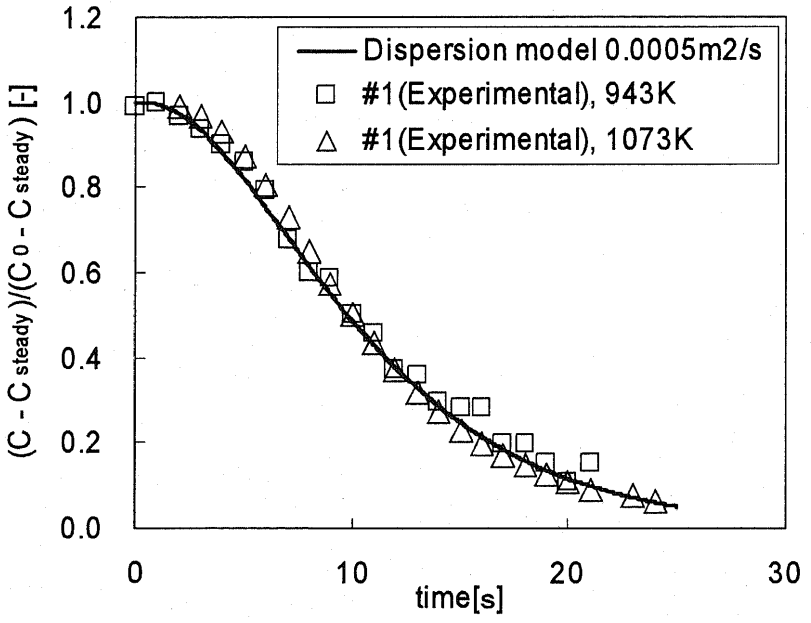

Fig. A2-1. Transient change in CO concentration for probe #1 after removing the shutter.

The one-dimensional diffusion model with a value of D_h = 0.0005 m^2/s also agreed with the experimental results of probe #2, #3 and #4 similarly to results for probe #1.

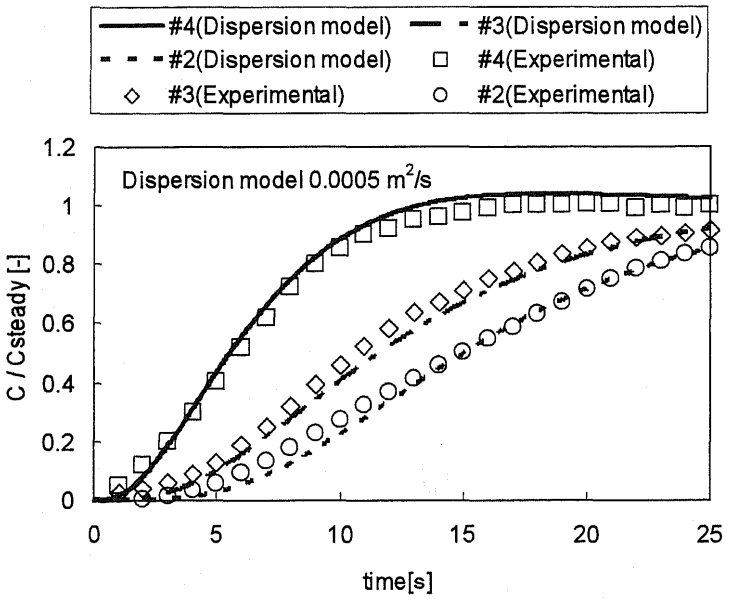

Fig. A2-2. Transient change in CO concentration for probes #2, #3, and #4 after removing the shutter.

For batch injection of activated carbon, a horizontal dispersion coefficient of 0.0003 m^2/s was found to match the experimental results.

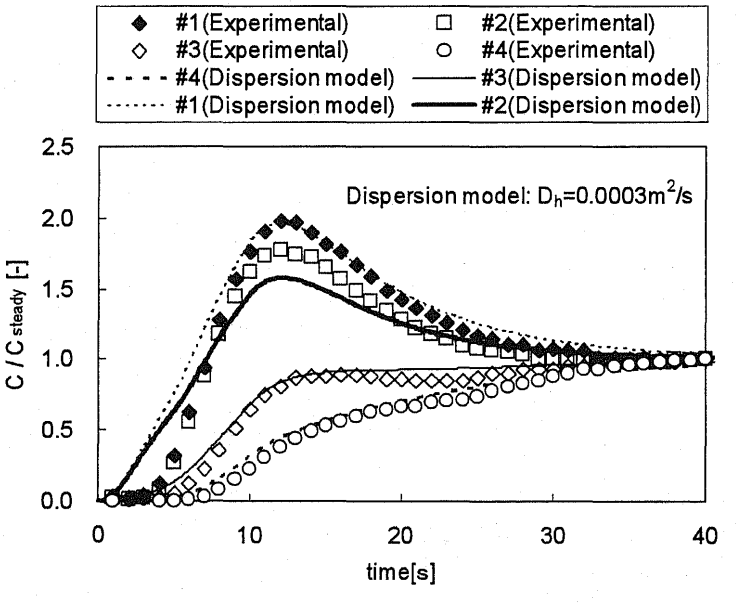

Fig. A2-3.Transient change in CO concentration at different horizontal position after batch injection of activated carbon.

APPENDIX A3

Horizontal concentration profile of CO_2 in two-dimensional bubbling fluidized bed without gas mixing effect.

The carbon concentration profile without taking account of gas mixing is shown in Fig. A3-1. The value D*h* of 0.003 m^2/s gives well correlated with the experimental results.

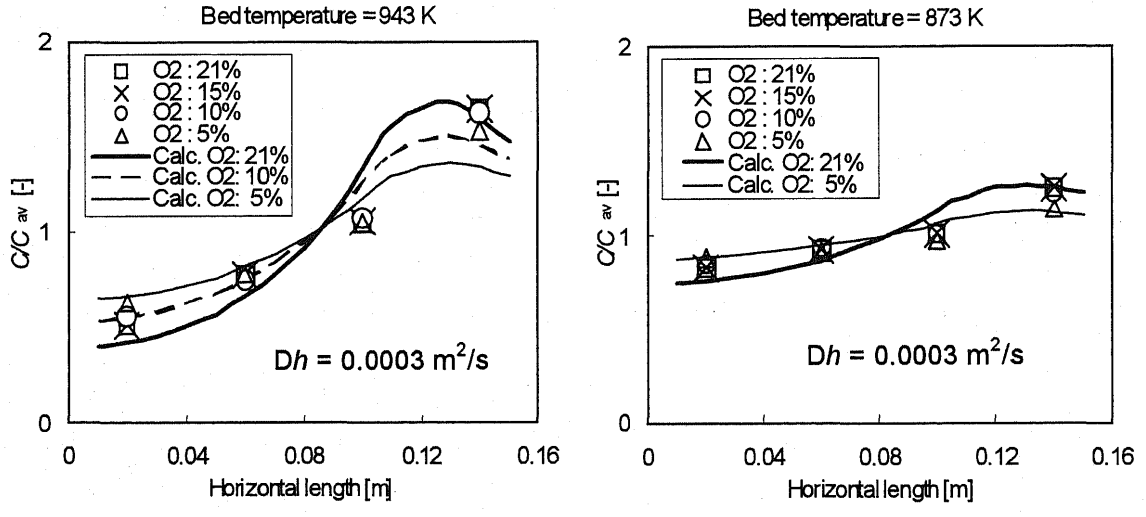

Fig. A3-1. Comparison of experimental results and those of the two-dimensional model.

The comparison is also made to correlation of dispersion coefficient models reported in the literatures as shown in Fig. A.3-4. For comparison of dispersion coefficients of 0.00016 m^2/s and 0.00068 m^2/s, it is found more uniform horizontal concentration profile at higher dispersion coefficients and for lower oxygen concentration.

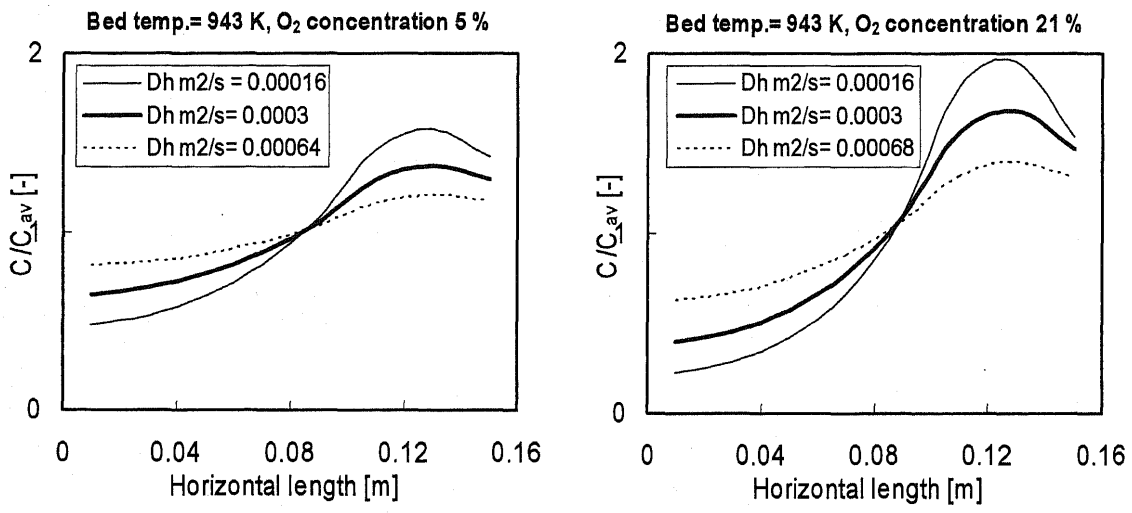

Fig. A3-2. Comparison of the present two-dimensional model and the published dispersion coefficient model

ACKNOWLEDGEMENT

Without help, support, and encouragement from several persons, I would never have been able to finish my study. It is a pleasant moment now to express my gratitude for all of them.

Foremost I would like to thank my supervisor Dr. Tadaaki Shimizu, for his inspiring and encouraging way to guide me to a deeper understanding of knowledge work, and his invaluable comments during the whole works of my PhD. program. I am glad to find an advisor who always kept on the progress of my works and always available when I needed his advises. His mentorship and his wide knowledge were essential to the completion of my study.

My thanks and gratitude are also extended to the members of committee; Dr. Kazuaki Yamagiwa, Dr. Isao Kimura, Dr. Masato Tanaka and Dr. Nobuyuki Fujisawa, for reading earlier versions of this thesis and providing many valuable comments that improved the presentation and contents of this work.

I am further indebted to all my lab mates for being good tutors and friends made it a convenient place to work. Particularly, I would like to thank Mr. Yousuke Nonaka for his work contribution of Chapter 4, Mr. Daisuke Yamada who contributed his worked for Chapter 3 and 4. A countless thank Mr. Masanori Toyono and other fellows of graduate and undergraduate students for their helps during the experiments.

I would like to express my deeply gratitude to Udayana University of Bali through the Rector and the Vice Rector of Academic Affairs for granting of leave to finish my Doctorate program in Niigata University of Japan. The financial support of this thesis by Japanese government through Mombukagakusho scholarship is gratefully acknowledged. Without their support, my ambition to study in Japan can

hardly be realized. The work of chapter 3 was also financially contributed by the Hatekayama Foundation.

Additional power for this study was also provided externally through my involvement in several social activities. Here, I would also like to gratefully acknowledge the support of some very special individuals. I wish to thank Mr. Ishikawa and his wife for their friendship. An extended thanks Mrs Sato and family for their homestay. I am indebted to Hai, Hui, Marlaw, Miyako, Phides, Kanako, Katia, Sum, Rey, Vanna and Indonesian student association in the period of April 2004 to March 2008 for their friendship with their uncountable fun activities.

My special acknowledge is due to all my family; bapak Wak, mamak Wak , kak Nik , wik Ajus, pak Tita, Uming, mbok Tu, mbok Ade, mbok Oming, dik Vika, bli Wi, mbok Yan, kak Uya, kak Tirta, mang Febi, bli Dek, mbok Wi, wik Ardy and mang Gita for their supports and cares. My parents bapak and mek Mangku for their encouragement and everlasting loves. My parents in law cak Nuk and mek Nuk for providing me a special hot spicy till the end of my study. There is no suitable word that can fully describe their deepest gratitude and loves. I owe my loving thanks to my wife mama Ocha and my son dik Ocha who was born with absent of me. They have lost a lot due to my study abroad. Without their unplugging love, patience, encouragement and understanding it would have been impossible for me to finish this work.

Above all, it would be definitely incomplete if I would forget to thank the Supreme Spirit of Ida Sang Hyang Widhi Wasa for everything.

Niigata, March 2008.

I Nyoman Suprapta Winaya